

Physics as a Function of
Energy & Luminosity

John Ellis
CERN Geneva

Invited Talk at the ICFA Seminar

KEK, Japan

May 1984

Introduction

You have already heard from Valentin Zakharov [1] about some of the ideas currently discussed by theorists, and some of the motivations they offer for expecting new physics in the range of mass up to $O(1)$ TeV. In this talk I plan to go into more detail about rates, signatures and backgrounds for these new physics possibilities. Most of my remarks concern hadron-hadron (hh) colliders, but I will also enter a plea on behalf of e^+e^- colliders. Most of the discussion on hh collider phenomenology is based on work done with Graciela Gelmini and Henrik Kowalski in preparation for the recent Lausanne workshop on a possible Large Hadron Collider in the LEP tunnel. Our work is described more completely in the Proceedings of that meeting, and you are referred there [2] for more details of the topics discussed here [3].

Section 2 of this talk contains some general comments on rates and final state distributions for new particle production in hh collisions. In particular, the average physics reaches of colliders with different centre-of-mass energies E_{cm} , luminosities L and beams (pp or $p\bar{p}$) are compared. Section 3 contains case studies of some of the possible new physics discussed by Zakharov, mainly Higgs bosons and supersymmetric particles, but also with a

few remarks about technicolor [4]. Section 4 summarizes these studies of new particle production at large hh colliders. Finally, Section 5 pleads the cleanliness of e^+e^- colliders [5] compared to hadron-hadron colliders, gives a guess as to the appropriate conversion factors between E_{cm} in e^+e^- and hh collisions [6], urges the complementarity of e^+e^- and hh colliders, and argues that a rational mix of world accelerators would include both species.

2. General Comments on Rates and Distributions.

Cross-sections for new heavy particle production in hh colliders have the general Drell-Yan [7] form

$$\sigma(x) = \int d\tau \mathcal{L}_{ab}(\tau) \hat{\sigma}_{ab}(X) \quad (1)$$

where $\hat{\sigma}_{ab}$ is the subprocess cross-section for partons of species a and b to collide to form the new state X (e.g., $\hat{\sigma}(\bar{q}q \rightarrow \tilde{g}\tilde{g})$), $\tau \equiv m_X^2/E_{cm}^2$ and \mathcal{L}_{ab} is the differential luminosity for collisions of partons of types a and b:

$$\mathcal{L}_{ab}(\tau) \equiv \int dx_a \int dx_b a(x_a) b(x_b) \delta(x_a x_b - \tau) \quad (2)$$

with x_a and x_b the fractions of the beam energies carried by the partons a and b respectively. Formulae (1) and (2) with the parton distributions scaled up [8] from present energies using the Altarelli-Parisi equations [9] may be approximately correct to within a factor of 2 for the production of particles with $m_X \gtrsim 0(10^{-2}) E_{cm}$, say $\gtrsim 0(100)$ GeV for hh colliders with $E_{cm} = 10$ to 40 TeV. Some typical parton-parton luminosity functions [8] for pp and $p\bar{p}$ collisions are shown in Fig. 1: they do not vary by very much in the range $10 \text{ TeV} < E_{cm} < 40 \text{ TeV}$. One generally expects a "geometric" form for the

subprocess cross-sections:

$$\hat{\sigma}(X) \cong \frac{1}{m_X^2} \times \begin{cases} 0(1) & \text{for strong processes} \\ 0(10^{-4}) & \text{for electroweak processes} \end{cases} \quad (3a)$$

$$(3b)$$

Fig. 2 shows some of the parton-parton luminosity functions of Fig. 1 multiplied by the geometric strong cross-section factor (3a). The next generation of hh colliders is expected [10] to have luminosities L in the range of $L=10^{32} \text{ cm}^{-2} \text{ sec}^{-1}$ ($p\bar{p}$?) to $10^{33} \text{ cm}^{-2} \text{ sec}^{-1}$ (pp ?), corresponding to an integrated luminosity of 10^{39} (10^{40}) cm^{-2} in a theoretical "year" of 10^7 seconds. We consider an "observable" cross-section to be one with $\geq 0(10^3)$ events in such a "year", corresponding to a cross-section $\sigma \geq 10^{-36} \text{ cm}^2$ ($p\bar{p}$?) to 10^{-37} cm^2 (pp ?), indicated by the dashed and dotted horizontal lines respectively in Fig. 2. We see that the physics reach of hh colliders with $E_{\text{cm}}=10$ to 40 TeV extends out to several TeV for strongly interacting particles, and 0(1) TeV for electroweak particles whose cross-sections (3b) are expected to be $0(10^{-4})$ smaller.

In more detail, we find [2] that between $E_{\text{cm}}=10$ and 40 TeV the attainable masses of strongly interacting particles produced by $u\bar{u}$ collisions increases as

$$m_X(\text{strong}) \propto E_{\text{cm}}^{0(1/2)} \quad (4)$$

In the range of luminosities between 10^{32} and $10^{33} \text{ cm}^{-2} \text{ sec}^{-1}$ we find that

$$m_X(\text{strong}) \propto \sqrt{s}^{0(0.2)} \quad (5)$$

while when comparing production by $u\bar{u}$ annihilation in pp and $p\bar{p}$ collisions

$$\frac{m_X(\text{strong}) | p\bar{p}}{m_X(\text{strong}) | pp} \cong 1.5 \quad (6)$$

Combining equations (5) and (6) we see that the physics reaches via $u\bar{u}$

annihilation in $p\bar{p}$ collisions at $L=10^{32} \text{ cm}^{-2} \text{ sec}^{-1}$ and pp collisions at $L=10^{33} \text{ cm}^{-2} \text{ sec}^{-1}$ are comparable, as can indeed be seen directly in Fig. 2. However, a higher luminosity pp collider has other advantages, notably for electroweak production mechanisms whose subprocess cross-sections are generally smaller (3b) and hence probe smaller values of τ where the $p\bar{p}$ and the pp parton-parton luminosity functions $\mathcal{L}(\tau)$ are very similar (see Fig. 1). Moreover, the parton-parton luminosities for gluon-gluon collisions are the same in pp and $p\bar{p}$, so their rates will always be larger in higher luminosity pp collisions. Therefore pp colliders are to be preferred.

It is a general consequence of the known parton distributions that "interesting" new heavy states tend to be produced centrally, typically with rapidities $|y| \leq 2$. Later we will see examples of this general rule in Higgs production and in the jet decays of gluinos [2]. In contrast, "boring" old light states tend to be produced forward, for example the rapidity distribution for W^\pm production extends [3] out to $|y| \leq 5$ as seen in Fig. 3, implying that 2/3 of the W^\pm decay within 5° of the beam-pipe. These remarks on final state distributions are summarized in the "Angle of Archaeology" [2] shown in Fig. 4. At any given hh collider, today's physics comes out at large angles to the beams, yesterday's physics at smaller angles, last week's physics at even smaller angles, etc., until palaeozoic physics such as elastic scattering is invisibly close to the beams. Physicists interested in different epochs can co-exist at different angles.

3. Case Studies of New Particle Production.

3.1 Higgs Production.

Several mechanisms for Higgs production are usually considered, starting with gluon-gluon fusion $gg \rightarrow H$ through virtual quark loops as in Fig. 5a [11].

The subprocess cross-section $\hat{\sigma}$ for this process is sensitive to the assumed heavy quark mass. If one only includes the t quark, $\hat{\sigma} \propto (m_t/m_H)^4$ for $m_t \ll m_H$. Curves [2] for $m_t=35$ GeV and 100 GeV are shown in Figs. 6a and 6b respectively. We see that if $m_t=35$ GeV the cross-section falls below the limit of "observability" of $0(1/10)$ pb for $m_H > 400(600)(800)$ GeV at $E_{cm}=10(20)(40)$ TeV. The reaction $gg \rightarrow H$ has the disadvantage of not possessing any final state signature beyond the Higgs decay products, which are predominately $\bar{t}t$ for $2m_t < m_H < 2m_W$ and predominately W^+W^- and Z^0Z^0 for heavier Higgses.

In contrast, the $\bar{q}q \rightarrow W^* \rightarrow W+H$ reaction [12] illustrated in Fig. 5b contains a spectator W in the final state, yielding $\bar{t}tW$ configurations if $2m_t < m_H < 2m_W$, and WWW if $m_H > 2m_W$. However, the cross-section is smaller than for the $gg \rightarrow H$ reactions, as can be seen in Fig. 7. The cross-section falls below the "observable" limit of $1/10$ pb for $m_H > 220(280)(360)$ GeV at $E_{cm} = 10(20)(40)$ TeV.

Another reaction mechanism with a final state event signature is $\bar{q}q$ or $gg \rightarrow \bar{t}tH$ as illustrated in Fig. 5c. A new complete calculation [13] gives the results shown in Fig. 8. For example $\sigma(\bar{t}tH) = 3$ pb for $m_t=35$ GeV and $m_H = 120$ GeV at $E_{cm} = 20$ TeV. Also shown in Fig 8 is a parallel background calculation [13], to which we return shortly.

The final reaction considered [14] is $WW \rightarrow H$, illustrated in Fig. 5d. This may be the most promising mechanism for $m_H > 0(400)$ GeV, and gives "observable" cross-sections above $1/10$ pb for all m_H in the expected range up to 1 TeV for $E_{cm} \geq 20$ TeV, as seen in Fig. 9. Unfortunately, like $gg \rightarrow H$ it does not have a clear signature to tag Higgs production events.

How observable is the Higgs? We expect [15] Higgs bosons with masses $0 < m_H < 0(100)$ GeV to have been detected at LEP before any large hh collider comes into operation. If $0(100) < m_H < 0(200)$ GeV, we expect $H \rightarrow \bar{t}t$ decay to dominate, and there to be an enormous background for $gg \rightarrow H$ or $WW \rightarrow H$ from simple gg or $\bar{q}q \rightarrow \bar{t}t$

production, and for $\bar{t}tH$ production from gg or $\bar{q}q \rightarrow \bar{t}t$ $\bar{t}t$ production [13] as seen in Fig. 8. However, the background to $\bar{q}q \rightarrow W^+H$ from $\bar{q}q \rightarrow \bar{t}tW$ seems [13] to be not much larger than the signal, and it may be possible to detect the Higgs via this reaction. If $0(200) < m_H < 0(400)$ GeV, we expect [16] $H \rightarrow W^+W^-$ and Z^0Z^0 decays to dominate, and the Higgs to have a total decay width much less than its mass. Unfortunately, the background reaction [17] $\bar{q}q \rightarrow W^+W^-$ or Z^0Z^0 , whose total cross-section is shown in Fig. 10 and whose $d\sigma/dm(W^+W^-)$ distribution is shown in Fig. 11, is larger than $gg \rightarrow H$ or $WW \rightarrow H$ in this mass range unless angular cuts are made. More optimistically, according to preliminary calculations, we do not expect large backgrounds to W^+H from WW production, or to $\bar{t}tH$ from $\bar{t}tWW$ production. If $0(400) < m_H < 0(1000)$ GeV we expect [16] the Higgs boson to be broad with $\Gamma(H \rightarrow W^+W^- + Z^0Z^0) \geq 1/10 m_H$. As seen in Figs. 7 and 8 we expect unobservably small cross-sections for W^+H or $\bar{t}tH$ production. Moreover, $\sigma(gg \rightarrow H) < \sigma(WW \rightarrow H)$ unless m_t is large. The broadness of the Higgs makes it difficult to detect $WW \rightarrow H$, unless we can suppress the $\bar{q}q \rightarrow W^+W^-$ background due to the W^+W^- cross-section at large $m(W^+W^-)$ (Fig. 11) using the sharp forward-backward peaking in the angular distribution (Fig. 12). Recall that the cross-section for $WW \rightarrow H$ falls relatively slowly for large m_H (Fig. 9), and that the spin-zero Higgs has an isotropic decay angular distribution.

Although complete background studies are not yet completed [18], it is clear that finding a Higgs boson at an hh collider will not be easy.

3.2 Supersymmetry Production.

Let us concentrate on the production of strongly ^{INTERACTING} integrating squarks \tilde{q} and gluinos \tilde{g} , since they have the largest cross-sections [19] in hh collisions.

As seen in Fig. 13, one calculates $\sigma(\tilde{g}\tilde{g})$ to be "observable", i.e., above $1/10$ pb, for $m_{\tilde{g}} \lesssim 1(1.6)(2.4)$ TeV at $E_{cm} = 10(20)(40)$ TeV. In most supersymmetric models [4] the \tilde{g} should decay into normal hadrons and a lighter photino,

probably $g \rightarrow q\bar{q}\tilde{\gamma}$. The photino, being neutral and weakly interacting, escapes from the apparatus much as a neutrino, thereby providing a large missing p_T signature: $p_T^{\text{miss}} = 0(m_{\tilde{g}}/3)$ as seen in Fig. 14. Figure 15 shows that the total $\tilde{g}\tilde{g}$ cross-section is not greatly reduced if one restricts to final states with

$$p_T^{\text{miss}} > 4\sigma: \quad \sigma = 0.7 \sqrt{E_T} \quad (7)$$

Where E_T is the total transverse energy in the event. The quantity σ in equation (7) is a guess at the resolution in p_T^{miss} based on experience with the UA1 detector. We see in Fig. (16a) that the rapidity distribution for q or \bar{q} jets from $g \rightarrow q\bar{q}\tilde{\gamma}$ is quite central, with

$$\langle y^2 \rangle^{1/2} = 1.1 \quad (8)$$

The average opening angle between jets is about 90° , and the p_T of the smallest p_T jet, whose distribution is shown in Fig. 16b, averages 140 GeV if $m_{\tilde{g}} = 1$ TeV. Thus $\tilde{g}\tilde{g}$ events giving 4-jet final states with large p_T^{miss} are quite different from conventional hh collider events.

Figure 17 shows [19] that $\sigma(\tilde{q}\tilde{q})$ should be "observable" with $\sigma > \frac{1}{10}$ pb for $m_{\tilde{q}} < 0.9$ (1.4)(2.0) TeV for $E_{\text{cm}} = 10$ (20)(40) TeV. Once again there is a large missing p_T signature, even if $\tilde{q} \rightarrow q\tilde{g}$ followed by $g \rightarrow q\bar{q}\tilde{\gamma}$. Shown in Fig. 18 is the p_T^{miss} signature for $\tilde{q} \rightarrow q\tilde{\gamma}$ decay: $p_T^{\text{miss}} = 0(m_{\tilde{q}}/2)$, which is even more impressive. We see in Fig. 19a that the rapidity distribution of jets from $\tilde{q}\tilde{q}$ production followed by $\tilde{q} \rightarrow q\tilde{g}$, $\tilde{g} \rightarrow q\bar{q}\tilde{\gamma}$ decay is quite central:

$$\langle y^2 \rangle^{1/2} = 1.2 \quad (9)$$

while the average of the minimum jet p_T distribution shown in Fig. 19b is about 90 GeV. The average angular distribution between the jets from

the $\tilde{q} \rightarrow q\tilde{g}$, $\tilde{g} \rightarrow q\tilde{q}\tilde{\gamma}$ decay chain is about 60° . It seems on the basis of these calculations that the final states containing 6 jets ($\tilde{q} \rightarrow q\tilde{g}, g \rightarrow q\tilde{q}\tilde{\gamma}$) or 2 jets ($\tilde{q} \rightarrow q\tilde{\gamma}$) with large missing p_T should also be quite distinctive.

A possible source of physics background is heavy $q\bar{q}$ production, e.g., $c\bar{c}$, $b\bar{b}$ or $t\bar{t}$, followed by semileptonic decay: $Q \rightarrow L\nu q$ in which the final state charged lepton is not seen. To escape detection, a decay muon would probably need $p_T^\mu < 5$ GeV while a decay electron would need $p_T^e < 50$ GeV unless it hid inside a jet. Such events give a p_T^{miss} vector which is almost parallel to one of the final state jets, with its momentum transverse to the jet axis $p_{TT} < m_Q/2 (m_t/2 \approx 20$ GeV?). By contrast, sparticle pair production gives a p_T^{miss} vector whose distribution is almost isotropic in the azimuthal angle ϕ , as seen in Fig. 20. It therefore seems likely that this physics background can be eliminated by a suitable cut in p_{TT} . There is also the instrumental background due to imperfect calorimeter energy resolution (7). However, the UAl collaboration [20] has already shown that it is possible to pick out and work with a small event sample having $p_T^{\text{miss}} < 4\sigma$ (7). This should be even easier at higher energies, since $E_T = 0(m_{\tilde{g}})$ in equation (7) implies

$$\frac{\sigma}{m_{\tilde{g}}} \propto \left(\frac{1}{m_{\tilde{g}}} \right)^{1/2} \quad (10)$$

while one expects $p_T^{\text{miss}} = 0(m_{\tilde{g}}/3 \text{ or } m_{\tilde{q}}/2)$.

It should be relatively easy to detect strongly interacting sparticles weighing up to $O(1)$ TeV at a large hh collider.

3.3 Technicolor

Shown in Fig. 21 are cross-sections for the production of neutral color octet technipions P_8^0 of mass ≈ 250 GeV [21], color octet technivectors V_8^\pm and V_8^0 of mass ≈ 900 GeV [20], and the techniquark continuum $Q_T\bar{Q}_T$, calculated [2]

for two guesses at the effective techniquark mass. We see that all the rates are large for $E_{\text{cm}} \geq 10$ TeV. Detectable signatures might include $P_8^0 \rightarrow \bar{t}t$ and $V_8^0 \rightarrow g+(\gamma \text{ or } Z^0)$, $V_8^\pm \rightarrow g+W^\pm$. There is a large background to $P_8^0 \rightarrow \bar{t}t$ from conventional $gg \rightarrow \bar{t}t$ [23]. Assuming an experimental resolution of $\pm 5\%$ in the $\bar{t}t$ invariant mass, we find [2]

$$\frac{\sigma(gg \rightarrow P_8^0 \rightarrow \bar{t}t)}{\sigma(gg \rightarrow \bar{t}t)} \approx \frac{1}{3} \quad (11)$$

This ratio can be improved [2] by making angular cuts, for example if one selects events with polar angle θ : $|\theta - \pi/2| < \pi/4$, then the signal-to-background ratio (11) becomes 1 to 1.

In view of the large cross-section shown in Fig. 21, it seems possible to detect technicolor at a large hh collider.

4. "Observability" of New Particles at hh Colliders.

On the basis of the case studies in section 3, we can pick out some important signatures one should be able to detect at a large hh collider.

$(\bar{t}t)$ pairs: These are useful in searches for Higgs bosons and for technipions.

Multiple W^\pm, Z^0 : These are important for heavy Higgs searches, and perhaps for technicolor searches. In view of the low rates for Higgs production, one would not like to pay the price of a leptonic decay branching ratio factor of a few percent for each W^\pm or Z^0 , and it would be desirable to have some efficiency for picking up W^\pm or $Z^0 \rightarrow$ dijets. It may be enough to be able to detect these in events where another W^\pm or Z^0 leptonic decay is used as a tag.

Missing p_T : Good resolution in p_T is essential for supersymmetric particle searches. Fortunately, the expected p_T^{miss} signature may be easier to detect

at higher energies, since $p_T^{\text{miss}} \propto m_{\tilde{g}}$, whereas the resolution $\sigma \propto m_{\tilde{g}}^{1/2}$.

Multijet mass bumps: Good multijet mass resolution is a necessity for the $(\bar{t}t)$, W^\pm and Z^0 searches whose necessity has already been mentioned.

γ -jet mass bumps: Good resolution here would be useful for technicolor searches as discussed in subsection 3.3, and also in limits for excited quarks (24) (not discussed here).

Charged leptons e, μ, τ, \dots : Good efficiency for detecting these is clearly a sine qua non for many of the other searches discussed above. It is also desirable as a veto for hunts for supersymmetry via missing p_T .

How difficult would it be to find at an hh collider the "expected" new particles discussed here? A preliminary conclusion is that *supersymmetry* would be relatively easy, *technicolor* would be possible, and a conventional *Higgs boson* would be relatively difficult, though not impossible.

The physics reaches of different possible hh colliders are summarized in Tables 1, 2 and 3. Table 1 indicates with what colliders one could be sure of producing an "observable" number of Higgses in all the mass range up to 1 TeV.

Table 2 summarizes the physics reaches for gluinos (squarks) as functions of E_{cm} and L.

Finally, Table 3 summarizes the "observability" of the cross-sections for technipion and technivector production for different E_{cm} and L.

Needless to say, the selection of new physics discussed here is purely a reflection of personal prejudice. Others are free to consider the observability of their own favorite particles at different hh colliders. Others are also free to decide how much they are prepared to pay in time and/or money for the higher energy and/or luminosity hh colliders listed in the Tables.

5. Comparison between e^+e^- and hh colliders.

Such a comparison [6] can only be based on subjective criteria which are

different for different physicists. It is as well to state one's basic assumptions as axioms which one does not attempt to derive. My first axiom is:

Axiom 1: e^+e^- collisions are cleaner than hh collisions.

I believe this to be true because the E_{cm} is better determined for e^+e^- collision than for parton-parton scattering in hh collisions, and because there are no "minimum-bias" or multiple interaction backgrounds in e^+e^- . Also, it is in my judgement very difficult to detect a heavy new electroweakly interacting particle such as a slepton in hh collisions, though it easy in e^+e^- collisions. Many physicists would accept axiom 1, but then ask pointedly: what E_{cm} in e^+e^- corresponds to what E_{cm} in hh? My answer [6] is in Table 4. I have taken an arbitrary "basket" of different "interesting" physics processes, calculated the equivalent E_{cm} in e^+e^- required to obtain the same reach in mass as at a given hh collider, displayed the corresponding $E_{cm}(e^+e^-)/E_{cm}(hh)$ ratio, and finally taken the geometric mean of all the calculated ratios. I conclude that, on the average,

$$\begin{aligned} E_{cm}(hh) = 10 \text{ TeV} &\leftrightarrow E_{cm}(e^+e^-) = 2 \text{ TeV} \\ E_{cm}(hh) = 40 \text{ TeV} &\leftrightarrow E_{cm}(e^+e^-) = 4 \text{ TeV} \end{aligned} \tag{12}$$

The different ratios in the bottom line of Table 4, and the resultant relatively slow increase in $E_{cm}(e^+e^-)$ (12), relect the previous claim (4) that the effective physics reach in hh collisions rises like $E_{cm}^{0(1/2)}$, while the physics reach in e^+e^- collisions rises like E_{cm} . A second pointed question is: when could an e^+e^- collide with $E_{cm} = 2$ to 4 TeV be built? Would it be slower than an hh collider with $E_{cm} = 10$ to 40 TeV, or could it be on a similar time-scale? Answers [5] will be provided tomorrow by Richter and by Skrinsky. In the discussions of the next few days, I urge that another axiom

be accepted.

Axiom 2: Large hh and e^+e^- colliders are complementary.

Because of this axiom, I do not advocate that all the next generation of large colliders be e^+e^- . It would be nice also to have an hh collider, although my axiom 1 would indicate that for comparable E_{cm} (12), e^+e^- colliders do better physics. It would probably be wiser to have a mix of large colliders in the 1990's: one e^+e^- with $E_{\text{cm}} \geq 2$ TeV, and one hh with $E_{\text{cm}} \geq 10$ TeV, plus other accelerators if we are very lucky.

References

1. V. Zakharov, these proceedings.
2. J. Ellis, G. Gelmini and H. Kowalski, Proceedings of the ECFA Workshop on the possibility of a Large Hadron Collider in the LEP tunnel, DESY preprint in preparation.
3. See also, E. Eichten, I. Hinchliffe, K.D. Lane and C. Quigg, Fermilab preprint (1984).
4. For recent reviews and references see J. Ellis, Proceedings of the 1983 SLAC Summer Institute on Particle Physics, ed. P. Mc Donough (SLAC, 1984); and CERN preprint TH-3802 (1984).
5. B. Richter, these proceedings; A. Skrinski, these proceedings.
6. For a previous such comparison, see J. Ellis, SLAC-PUB-3127 (1983).
7. S.D. Drell and T.-M. Yan, Phys. Rev. Lett 25, 316 (1970).
8. We use the distributions of W. Furmanski and H. Kowalski, Nucl. Phys. B224, 523 (1983).
9. G. Altarelli and G. Parisi, Nucl. Phys. B126, 298 (1977).

10. M. Tigner, these proceedings; G. Brianti, these proceedings.
11. H. Georgi, S.L. Glashow, M.E. Machacek and D.V. Nanopoulos, Phys. Rev. Lett. 40, 692 (1978).
12. S.L. Glashow, D.V. Nanopoulos and A. Yildiz, Phys. Rev. D18, 1724 (1978).
13. Z. Kunszt, University of Bern preprint (1984).
14. R.N. Cahn and S. Dawson, Phys. Lett. 136B, 196 (1984), E 138B, 464 (1984).
15. Exotic Particles Study Group, G. Barbiellini, et al., DESY preprint 79/27 (1979).
16. B.W. Lee, C. Quigg and H. Thacker, Phys. Rev. D16, 1519 (1977).
17. R.W. Brown and K.O. Mikaelian, Phys. Rev. D19, 922 (1979);
R.W. Brown, D. Sahdev and K.O. Mikaelian, Phys. Rev. D20, 1164 (1979).
18. For more discussion, see G.L. Kane, these proceedings.
19. G.L. Kane and J.P. L veill , Phys. Lett. 112B, 227 (1982);
P. Harrison and C.H. Llewellyn Smith, Nucl. Phys. B213, 223 (1982),
E B223, 542 (1982).
20. UA1 Collaboration, G. Arnison et al., Phys. Lett. 139B, 115 (1984);
see also UA2 Collaboration, P. Bagmia et al., Phys. Lett. 139B, 105
(1984).
21. S. Dimopoulos, Nucl. Phys. B168, 69 (1980).
22. S. Dimopoulos, S. Raby and G.L. Kane, Nucl. Phys. B182, 77 (1981).
23. G. Girardi, P. M ry and P. Sorba, Nucl. Phys. B195, 410 (1982).
24. A. De R jula, L. Maiani and R. Petronzio, CERN preprint TH-3779 (1983).

Figure Captions

1. Effective parton-parton luminosity functions [2] plotted in terms of $\sqrt{\tau}$. Note the similarity of the luminosities in pp and $\bar{p}p$ collisions for $\sqrt{\tau} \leq 0.1$ corresponding to $m_X \leq \frac{1}{10} E_{\text{cm}}$.
2. Some of the parton-parton luminosity functions of Fig. 1 multiplied [2] by a geometric cross-section factor $1/m_X^2$ [3]. The horizontal dashed (dotted) lines correspond to $\sigma = 1$ (1/10) pb above which cross sections should be observable with a hadron-hadron luminosity of 10^{32} (10^{33}) $\text{cm}^{-2} \text{sec}^{-1}$.
3. Rapidity distribution [3] for $pp \rightarrow W^+ + X$ at $E_{\text{cm}} = 40 \text{ TeV}$.
4. The angle of archaeology: today's physics emerges at wide angles, yesterday's physics emerges closer to the beam-pipe, last week's even closer, etc.
5. (a) Virtual quark loop diagram [11] for $gg \rightarrow H$;
(b) Diagram [12] for $\bar{q}q \rightarrow W^* \rightarrow W + H$;
(c) Diagrams [15] for $gg \rightarrow \bar{t}t + H$ and $\bar{q}q \rightarrow \bar{t}t + H$;
(d) Diagram [14] for $qq \rightarrow qqWW \rightarrow qqH$.
6. Cross-sections [2] for $gg \rightarrow H$ through t quark loops with $m_t = 35 \text{ GeV}$, 70 GeV and 100 GeV.
7. Cross-sections [2] for $W + H$ production.
8. Cross-sections [2,13] for $\bar{t}t + H$ production, together with ($\bar{t}t\bar{t}t$) backgrounds calculated for $m_t = 35, 70 \text{ GeV}$.
9. Cross-sections [2,14] for H production by WW fusion.
10. Total-cross sections [2] for W^+W^- production by $\bar{q}q$ collisions at hh colliders.

11. Invariant mass distributions [2] $d\sigma/dm(W^+W^-)$ for W^+W^- production.
12. Angular distributions [17] for W^+W^- pair production, in the centre-of-mass of the pair.
13. Cross-sections [2] for gluino pair production [19] at hh colliders.
14. Missing p_T signature [2] for $\tilde{g}\tilde{g}$ production followed by $\tilde{g} \rightarrow q\bar{q}\tilde{\gamma}$ decay.
15. Effect on the total cross-sections of Fig. 13 of restricting [2] to events with missing p_T : $p_T^{\text{miss}} > 4\sigma$ with σ given by Eq. (7).
16. (a) Rapidity distribution [2] for q and \bar{q} jets from $\tilde{g} \rightarrow q\bar{q}\tilde{\gamma}$ decay, for $E_{\text{cm}} = 20$ TeV, $m_{\tilde{g}} = 1$ TeV;
 (b) distribution [2] in p_T of the smallest jet p_{Tj} , for the same choices of E_{cm} and $m_{\tilde{g}}$.
17. Cross-sections [2] for $\tilde{q}\bar{\tilde{q}}$ pair production at hh colliders.
18. Missing p_T signature [2] for $\tilde{q}\bar{\tilde{q}}$ production followed by $\tilde{q} \rightarrow q\tilde{\gamma}$ decay.
19. (a) Rapidity distribution [2] of jets from $\tilde{q}\bar{\tilde{q}}$ production followed by $\tilde{q} \rightarrow q\tilde{g}$, $\tilde{g} \rightarrow q\bar{q}\tilde{\gamma}$ decay, assuming $m_{\tilde{q}} = 1$ TeV, $m_{\tilde{g}} = 0.7$ TeV, and
 (b) distribution [2] in p_T of the smallest p_T jet, for the same choice of parameters.
20. Distributions [2] in the projection of the missing p_T vector transverse to the closest observed jet from $\tilde{g}\tilde{g}$ production followed by $\tilde{g} \rightarrow q\bar{q}\tilde{\gamma}$ decay.
21. Cross-sections [2] for neutral color octet technipion P_8^0 , neutral color octet technicolor V_8^0 , charged color octet technivector V_8^\pm and technicolor continuum production.

$L(\text{cm}^{-2} \text{sec}^{-1})$	$E_{\text{cm}} (\text{TeV})$		
	10	20	40
$10^{32}(\text{pp}^-?)$	X	X	✓
$10^{33}(\text{pp}?)$	X	✓	✓

TABLE 1: "Observable" production of Higgses up to 1 TeV
in mass

$L(\text{cm}^{-2} \text{sec}^{-1})$	$E_{\text{cm}}, \text{ masses (TeV)}$		
	10	20	40
$10^{32}(\text{pp}^-?)$	0.6(0.6)	1.1(0.9)	1.8(1.3)
$10^{33}(\text{pp}?)$	0.9(0.9)	1.6(1.4)	2.4(2.0)

TABLE 2: "Observable" masses for gluinos (squarks)

$L(\text{cm}^{-2} \text{sec}^{-1})$	$E_{\text{cm}} (\text{TeV})$		
	10	20	40
$10^{32} (\text{pp}?)$	✓	✓	✓
$10^{33} (\text{pp}?)$	✓	✓	✓

TABLE 3: Technicolor "Observability"

Process	$E_{cm}^{hh} = 10 \text{ TeV}$	$E_{cm}^{hh} = 40 \text{ TeV}$
Jet pairs	0.44	0.28
$\mu^+ \mu^-$	0.09	0.03
heavy (s)lepton	0.09	0.03
heavy Z^0	0.23	0.15
heavy W^\pm	0.5	0.35
techni eta	0.2	0.08
gluino	0.24	0.12
heavy quark	0.14	0.07
geometric mean	0.2	0.1

(Ratios $E_{cm}(e^+e^-)/E_{cm}(hh)$ for selected reactions)

TABLE 4: Comparison of E_{cm} for e^+e^- and hh colliders

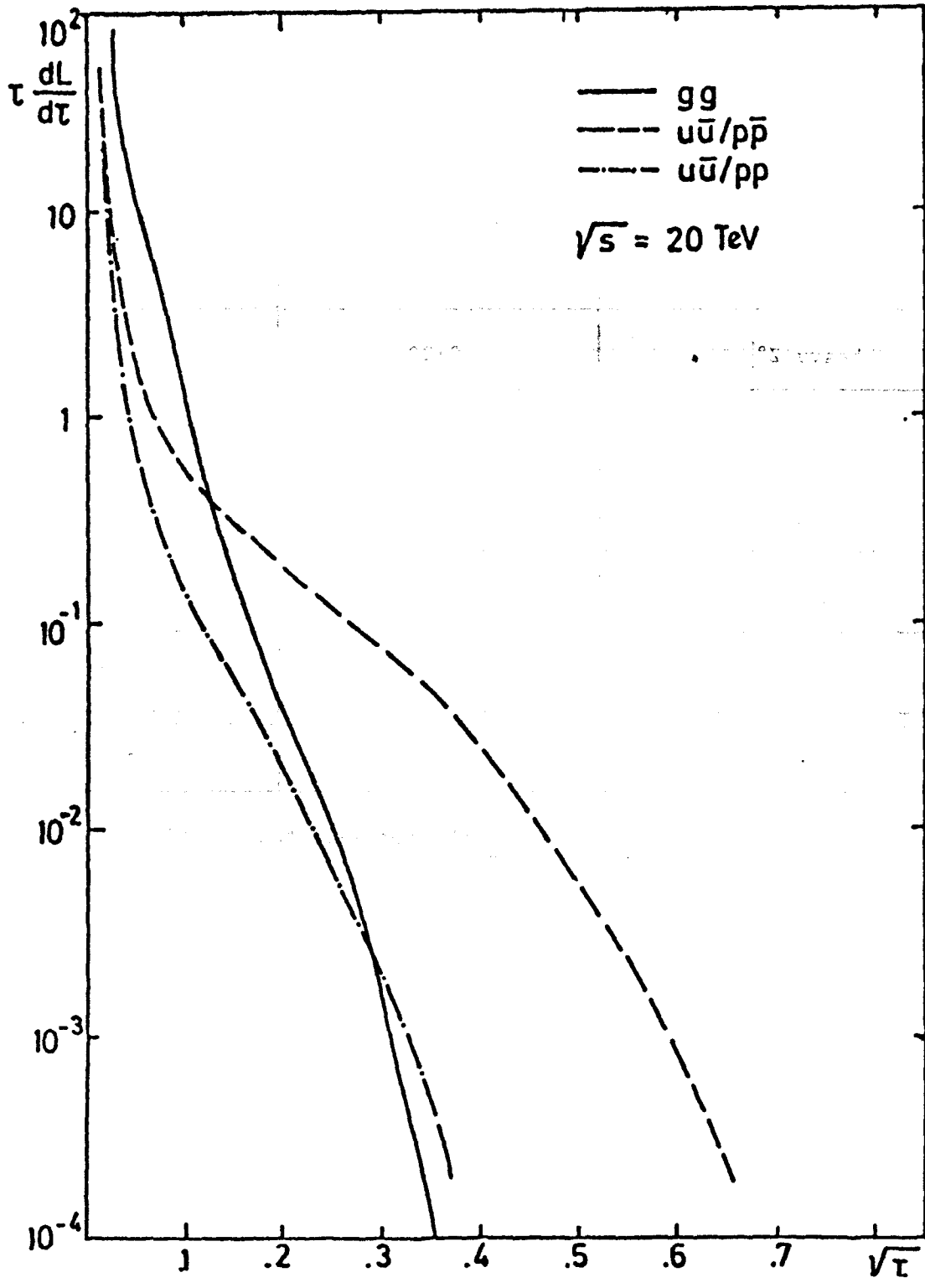


Fig. 1a

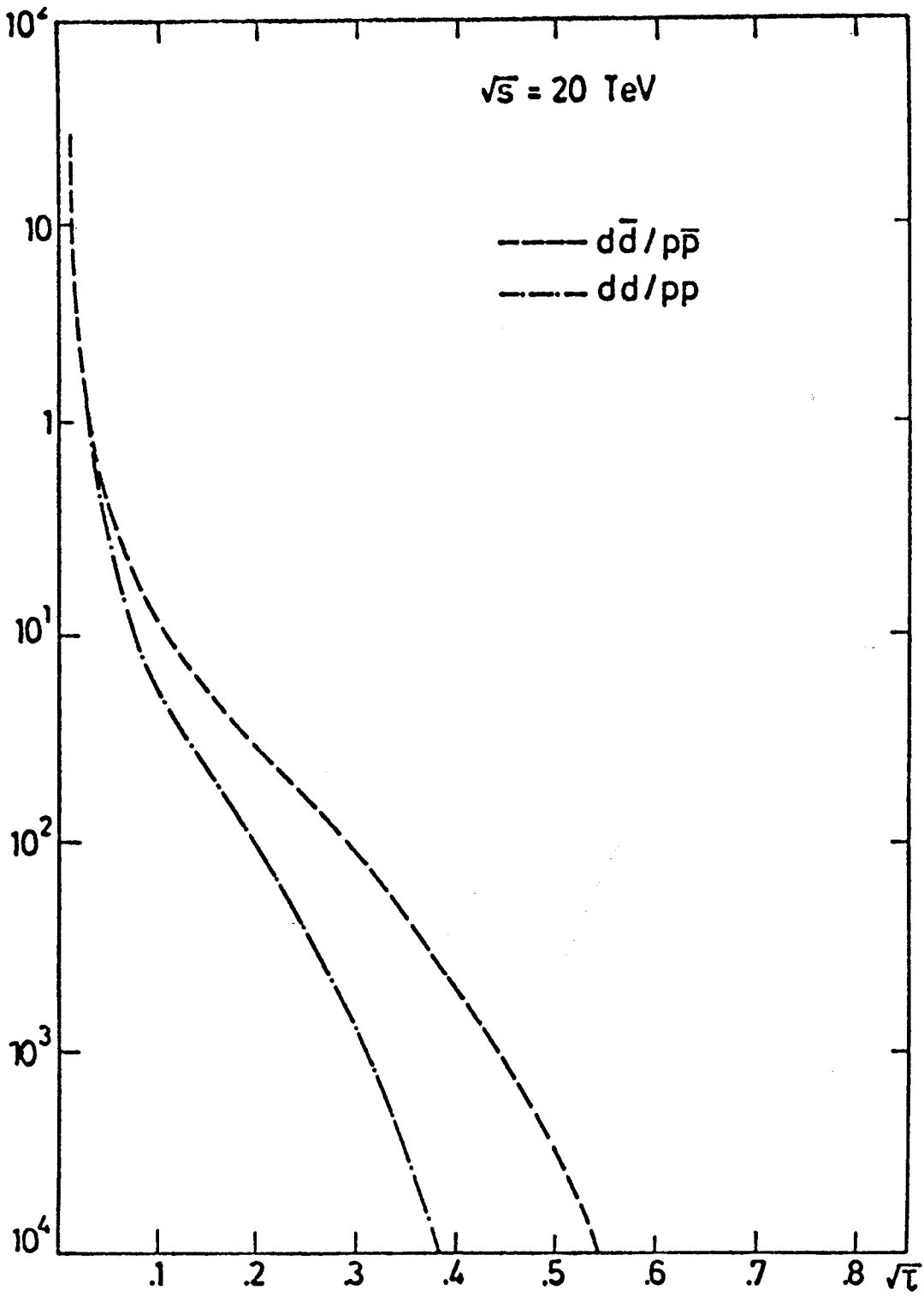


Fig. 1b

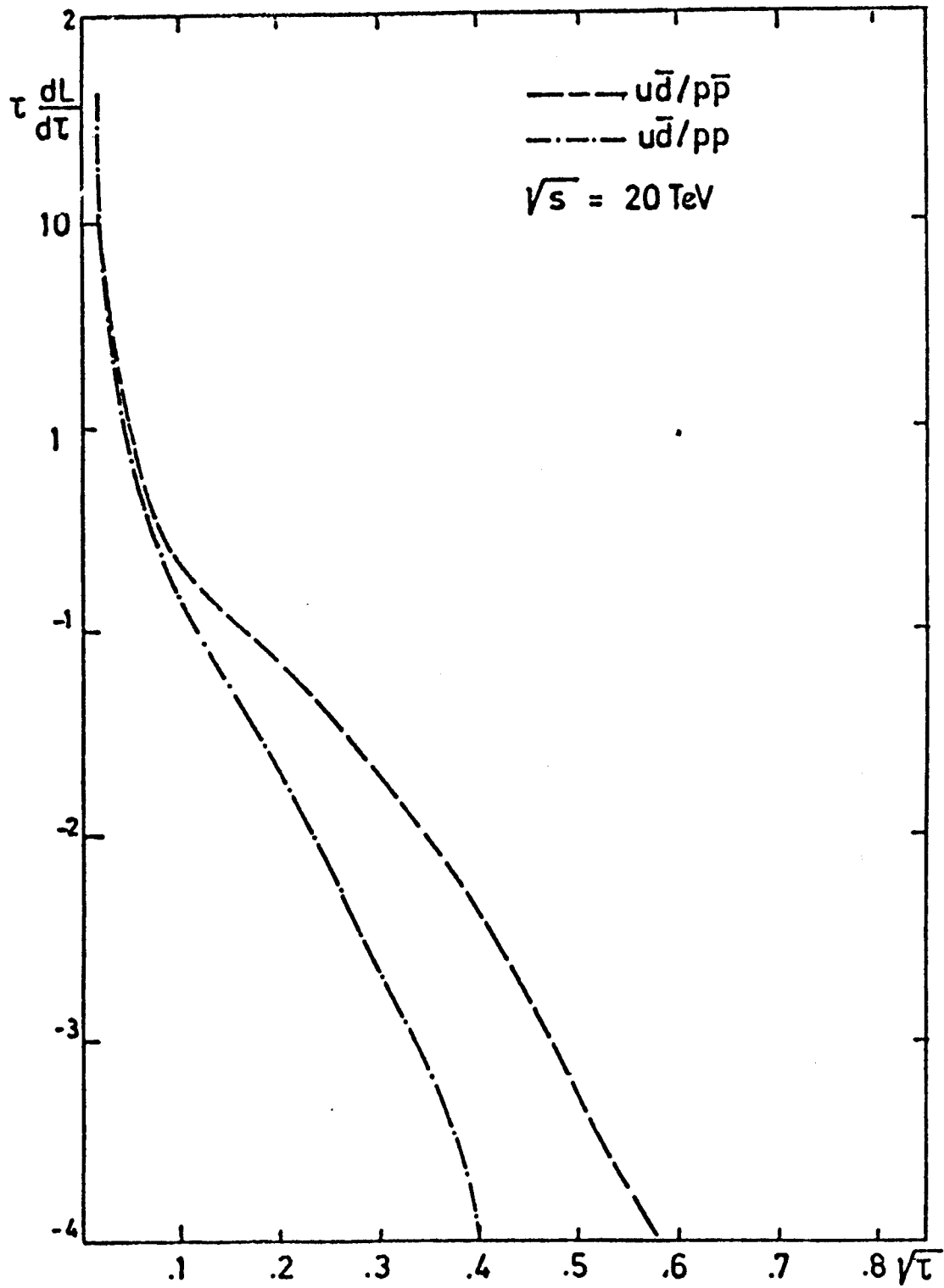


Fig. 1c

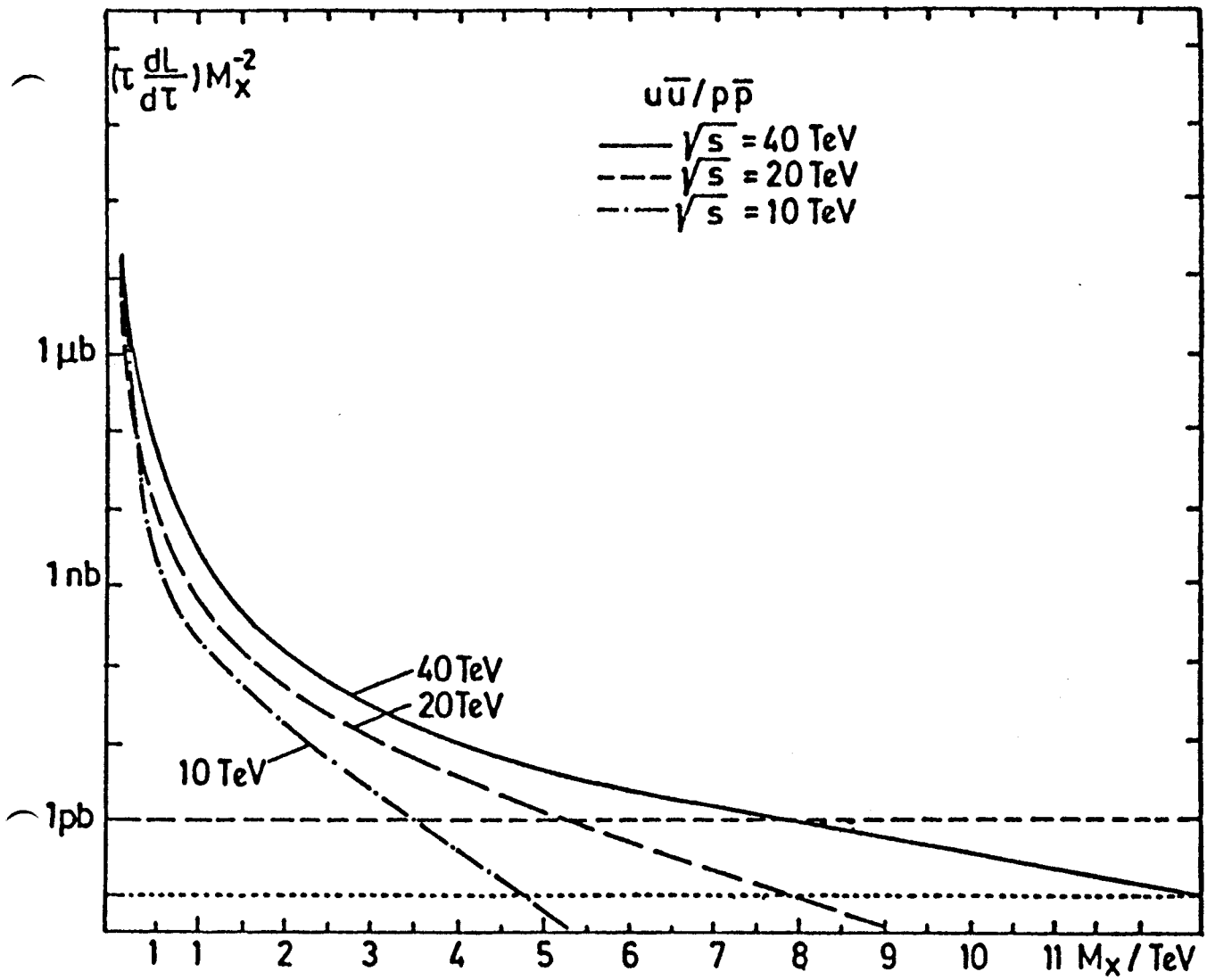


Fig. 2a

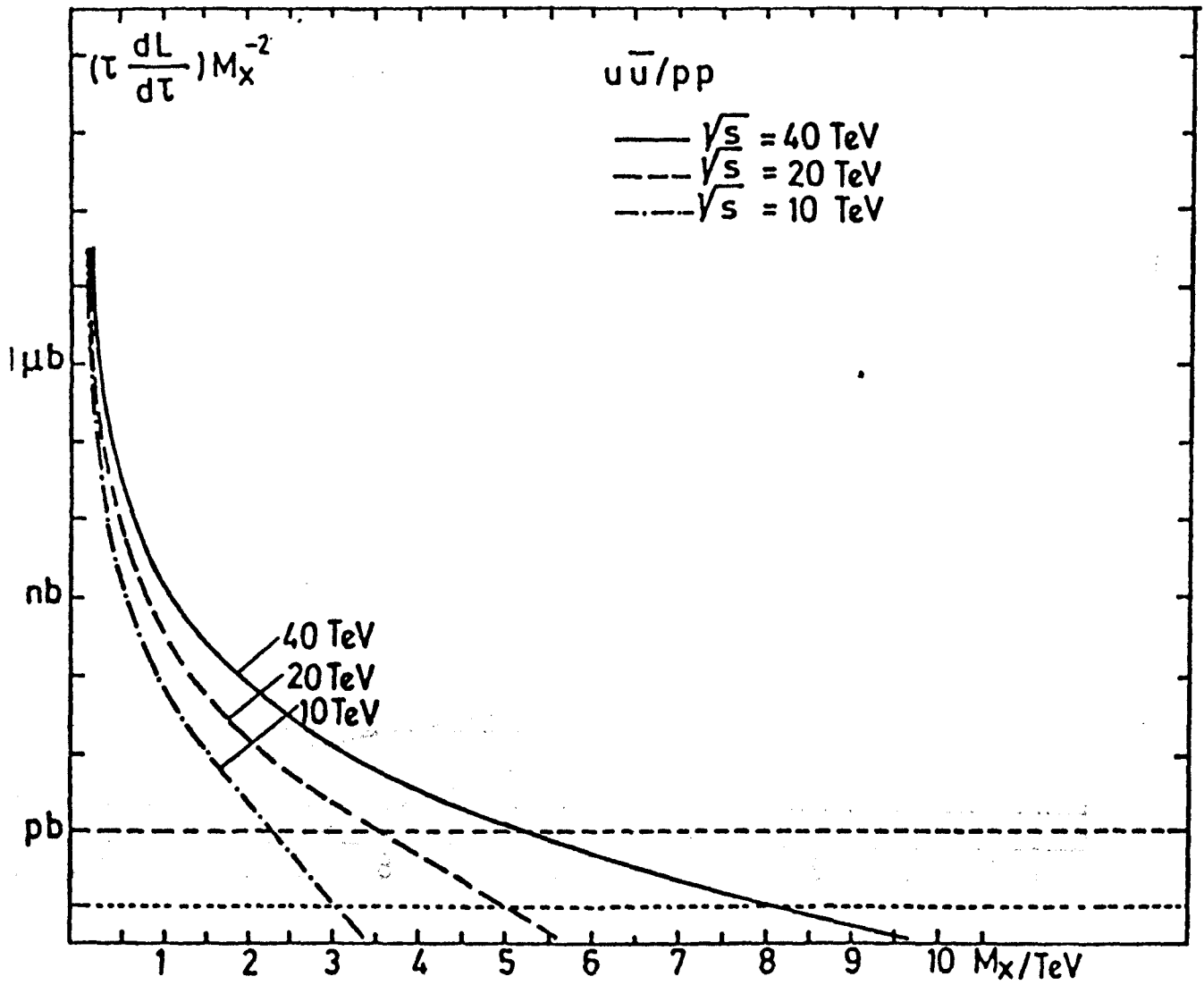


Fig. 2b

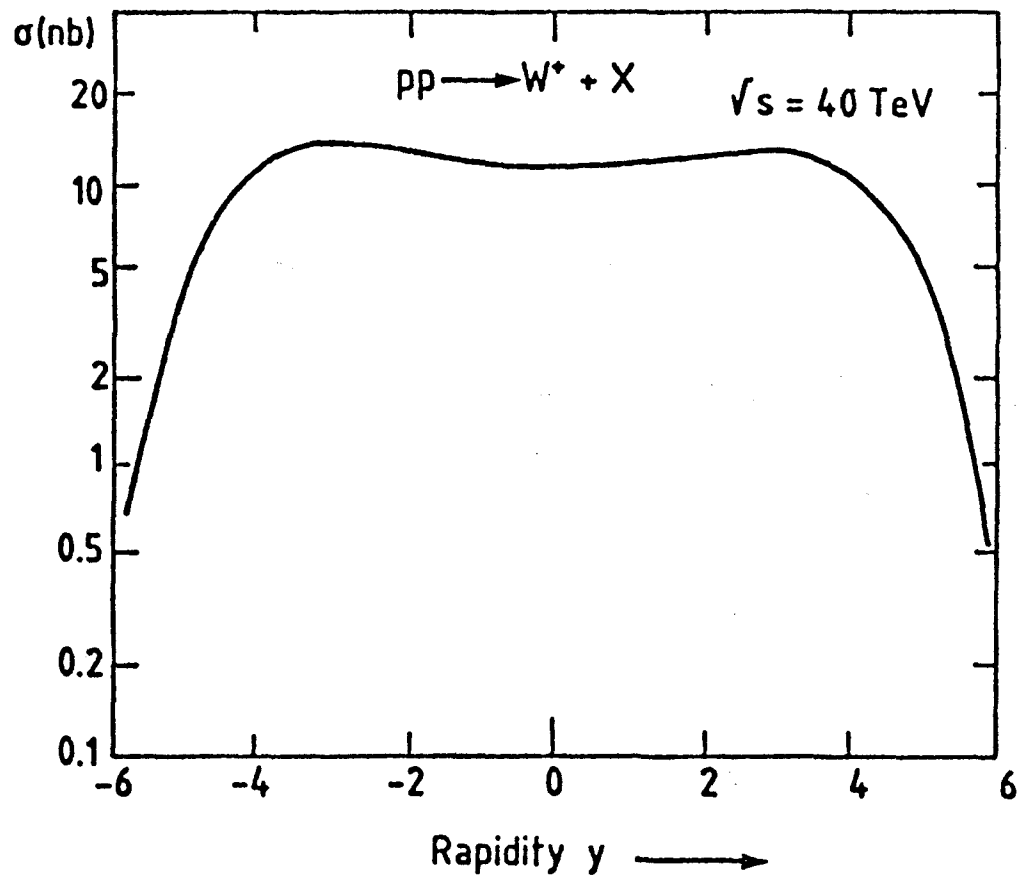


Fig. 3

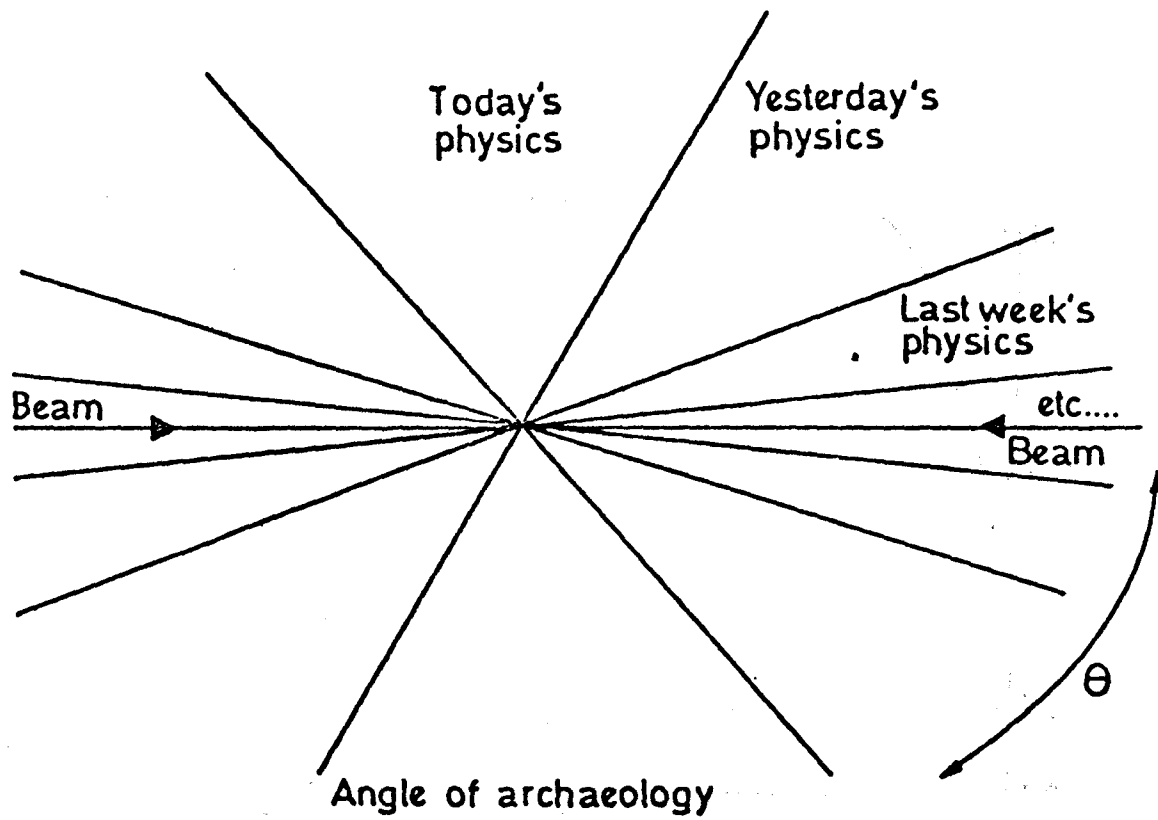


Fig. 4

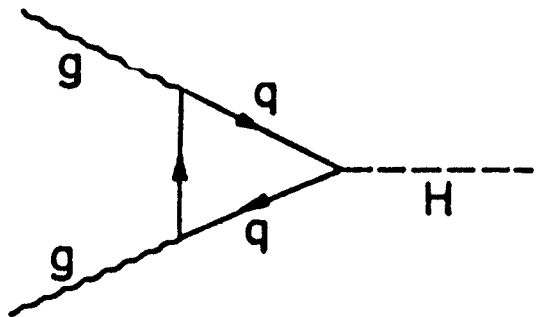


Fig. 5a

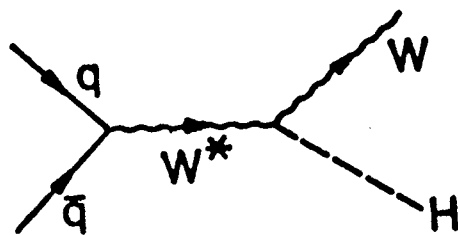
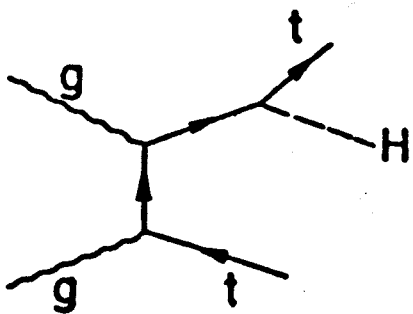


Fig. 5b



+ etc.

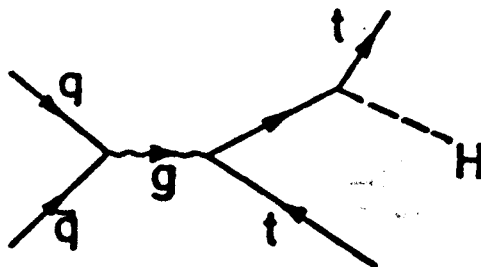


Fig. 5c

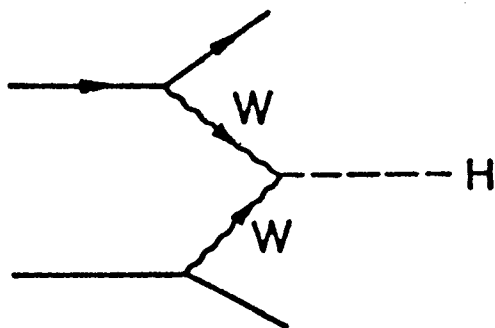


Fig. 5d

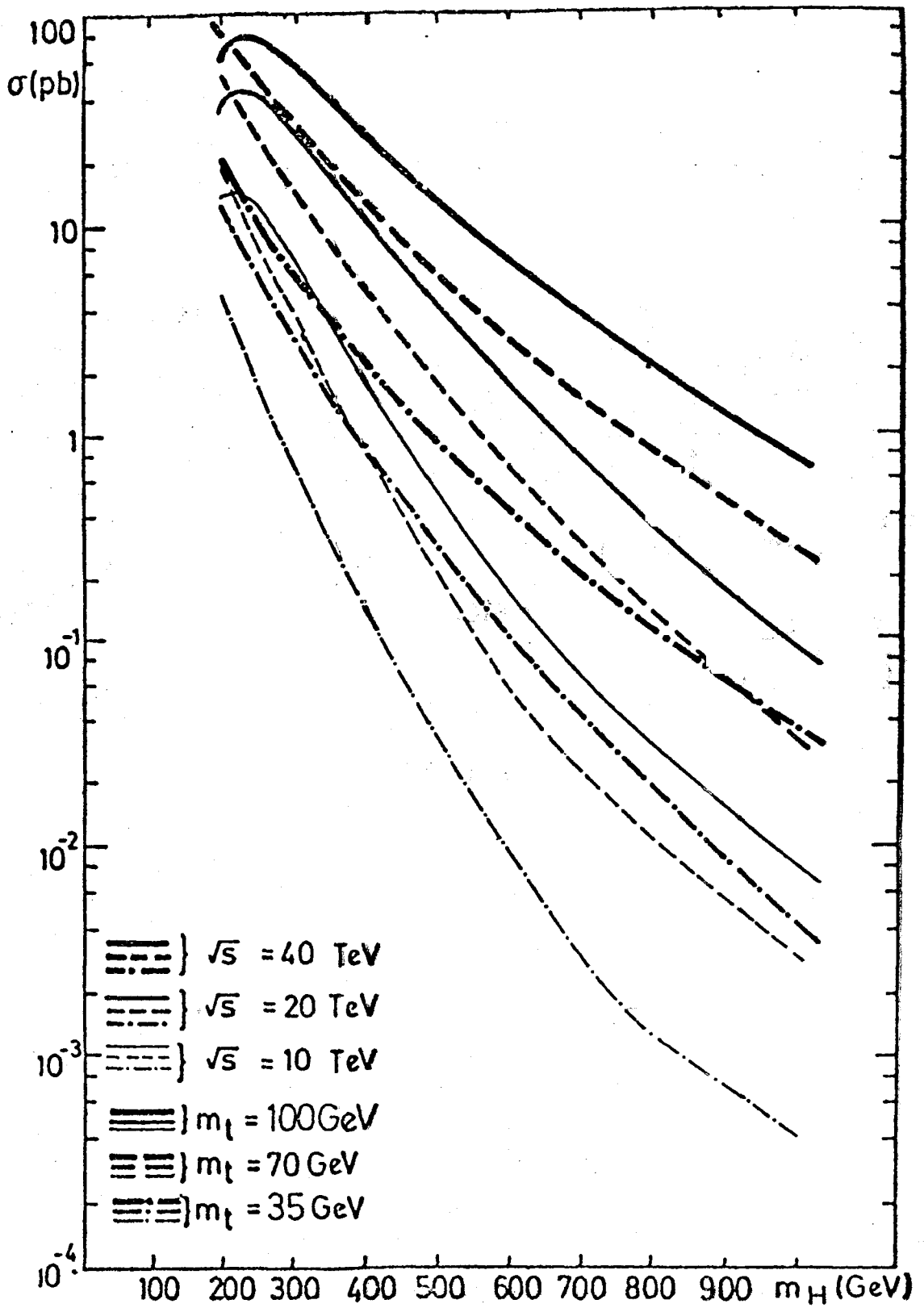


Fig. 6

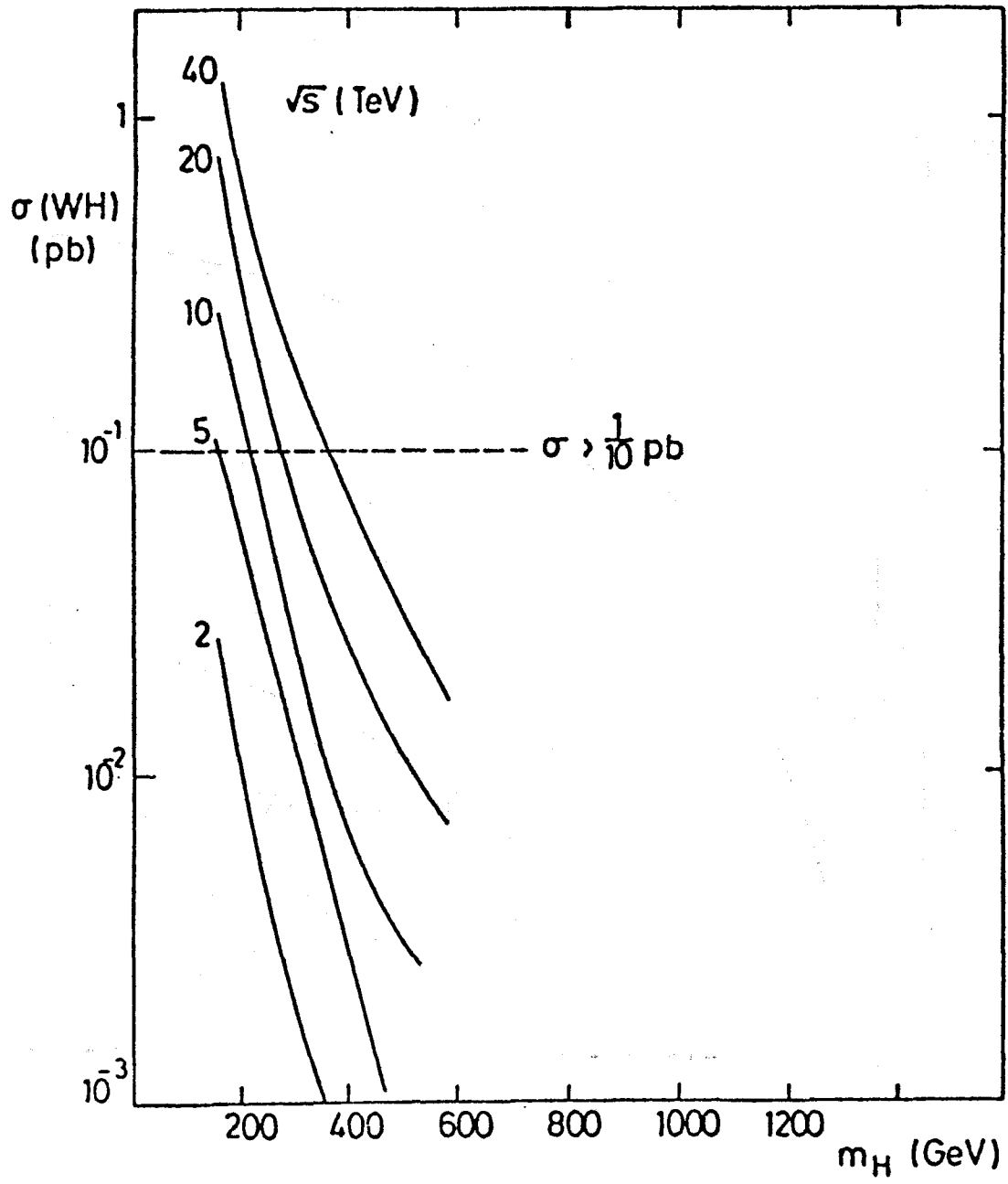


Fig. 7

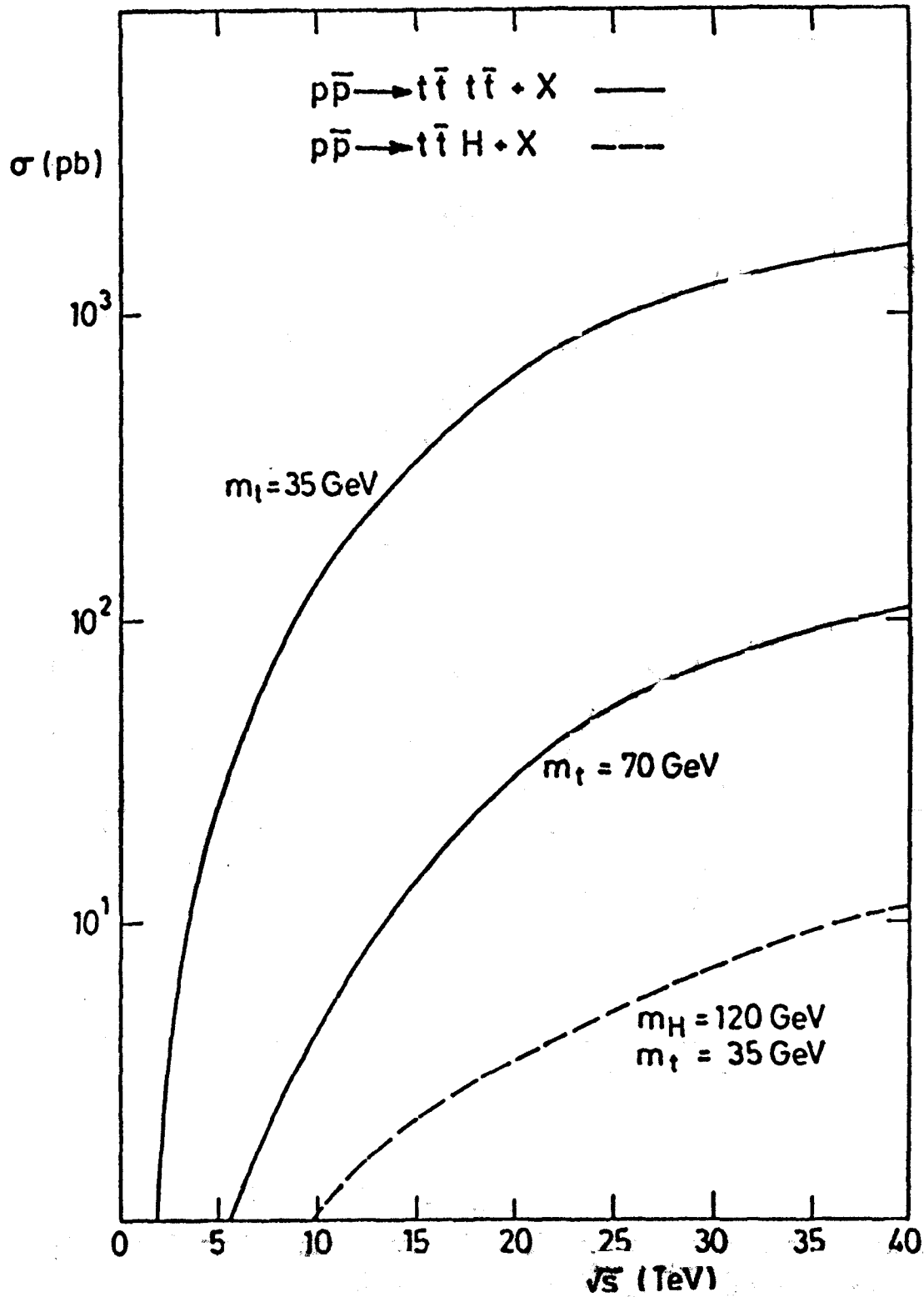


Fig. 8

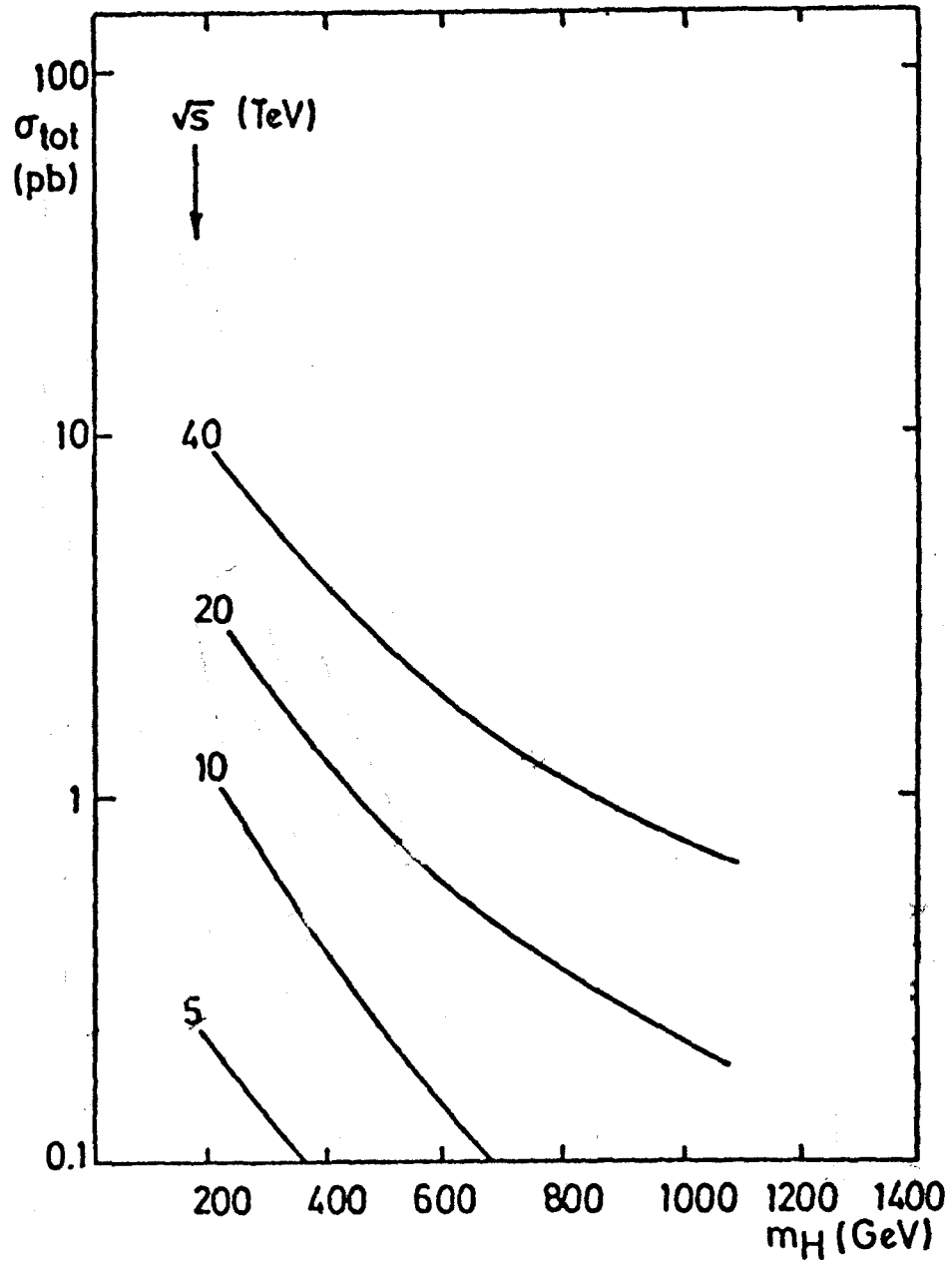


Fig. 9

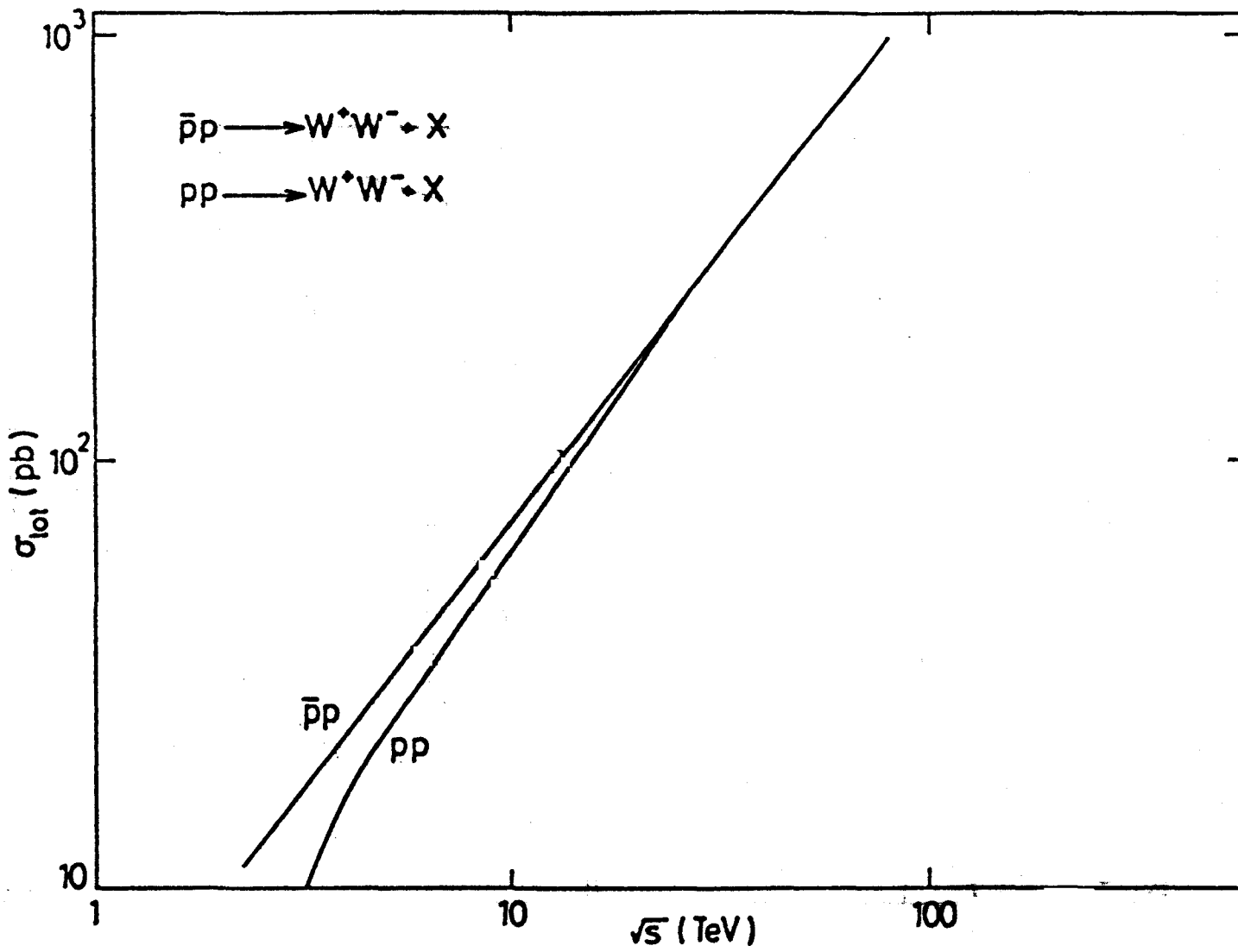


Fig. 10 \sqrt{s} (TeV)

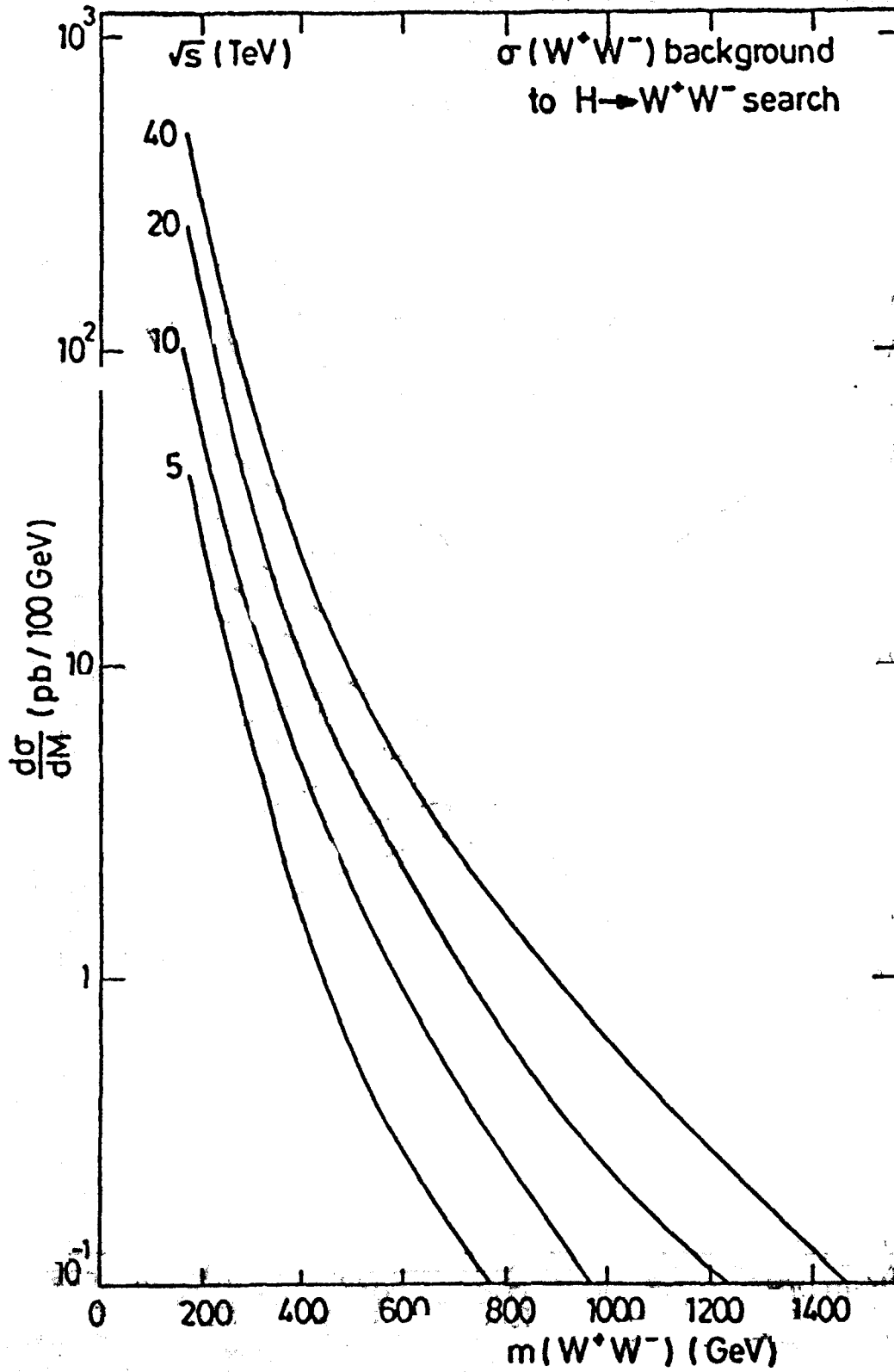


Fig. 11

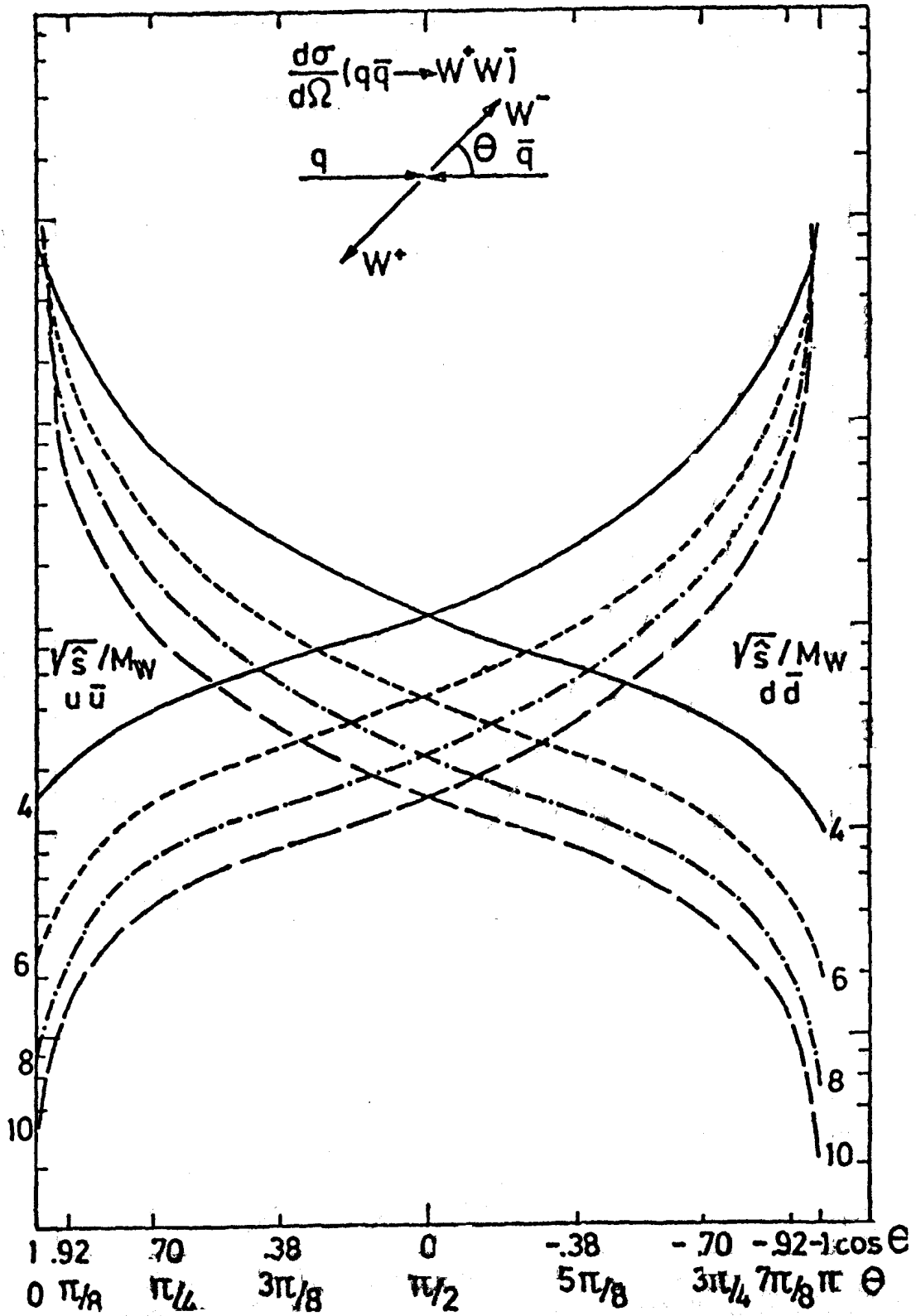


Fig. 12

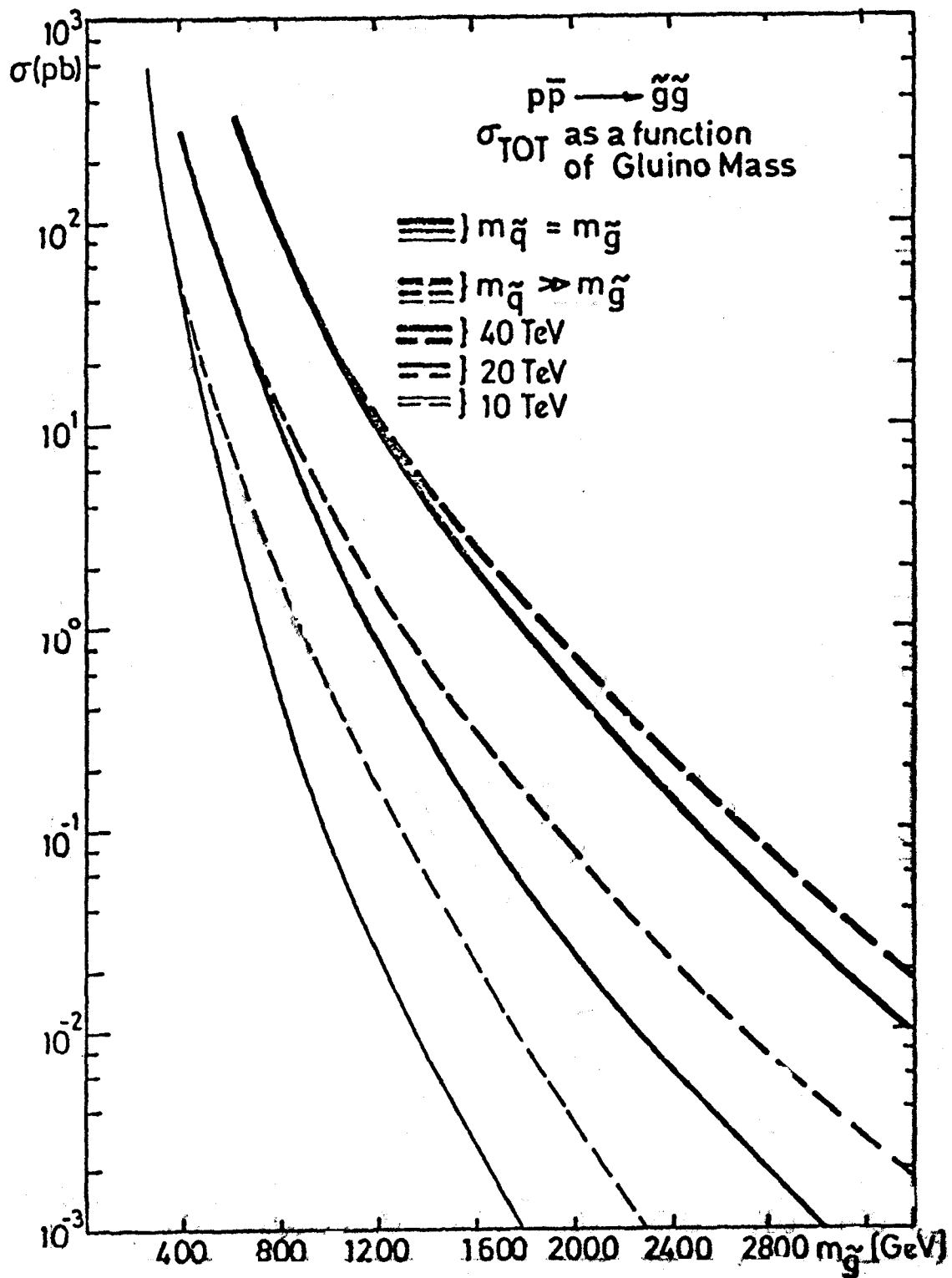


Fig. 13

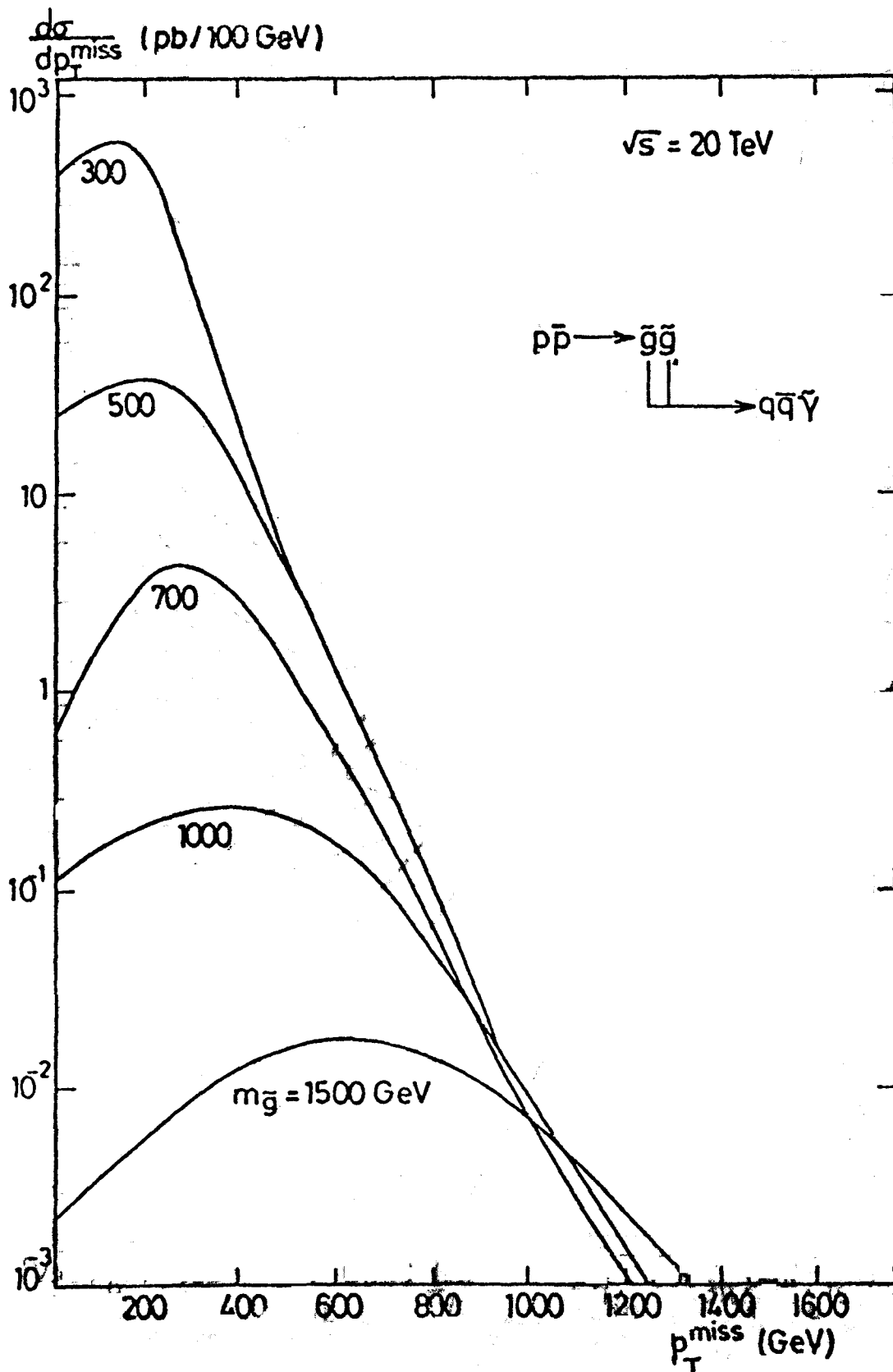


Fig. 14

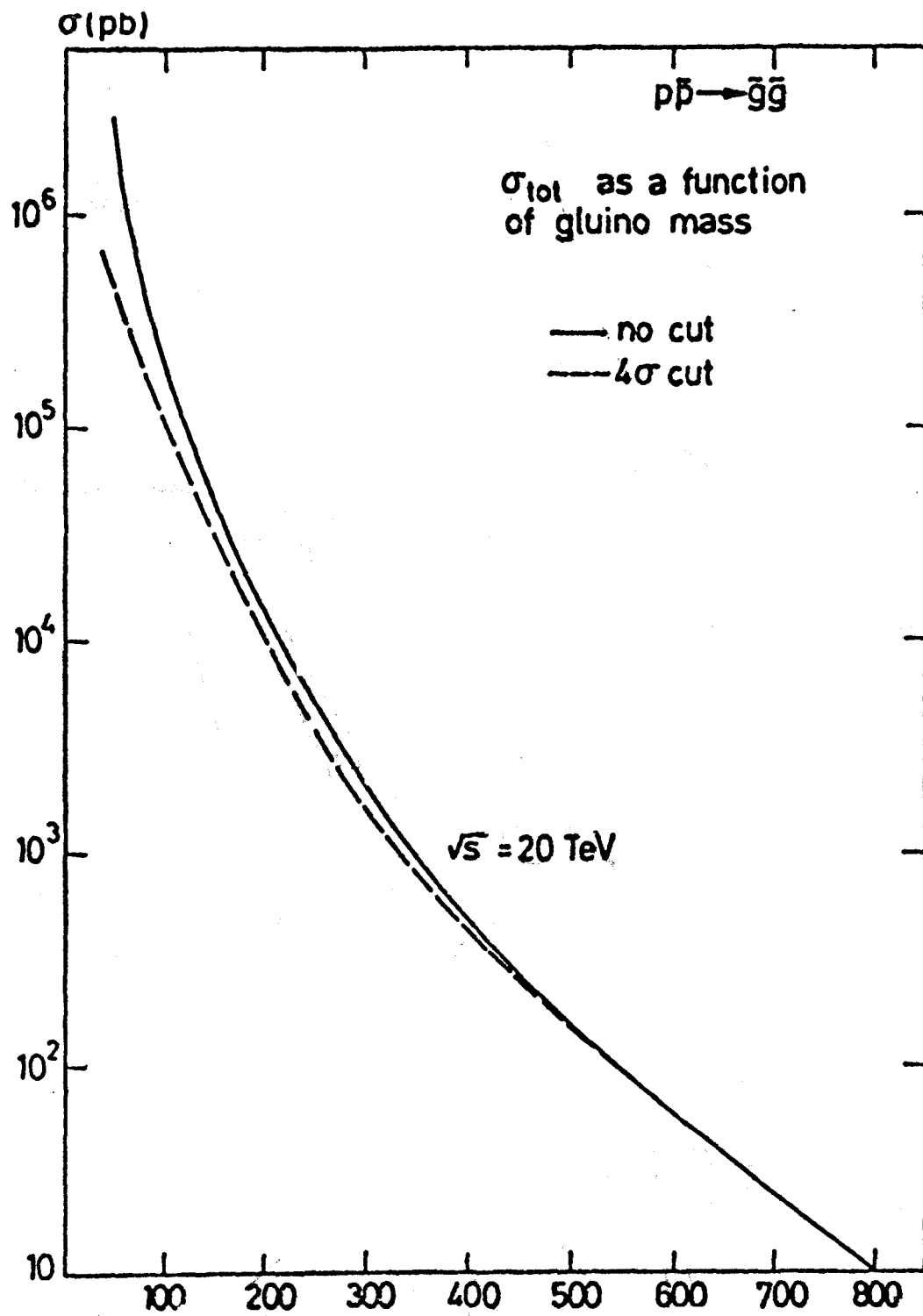


Fig. 15

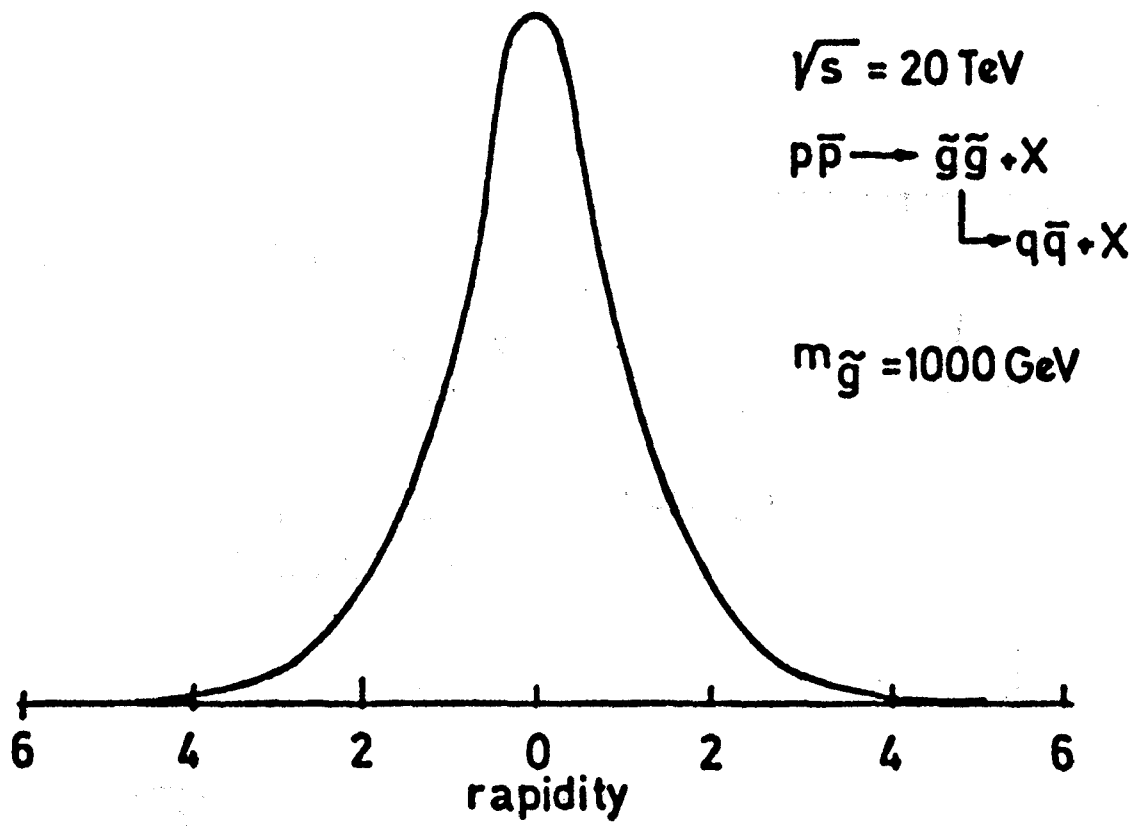


Fig. 16a

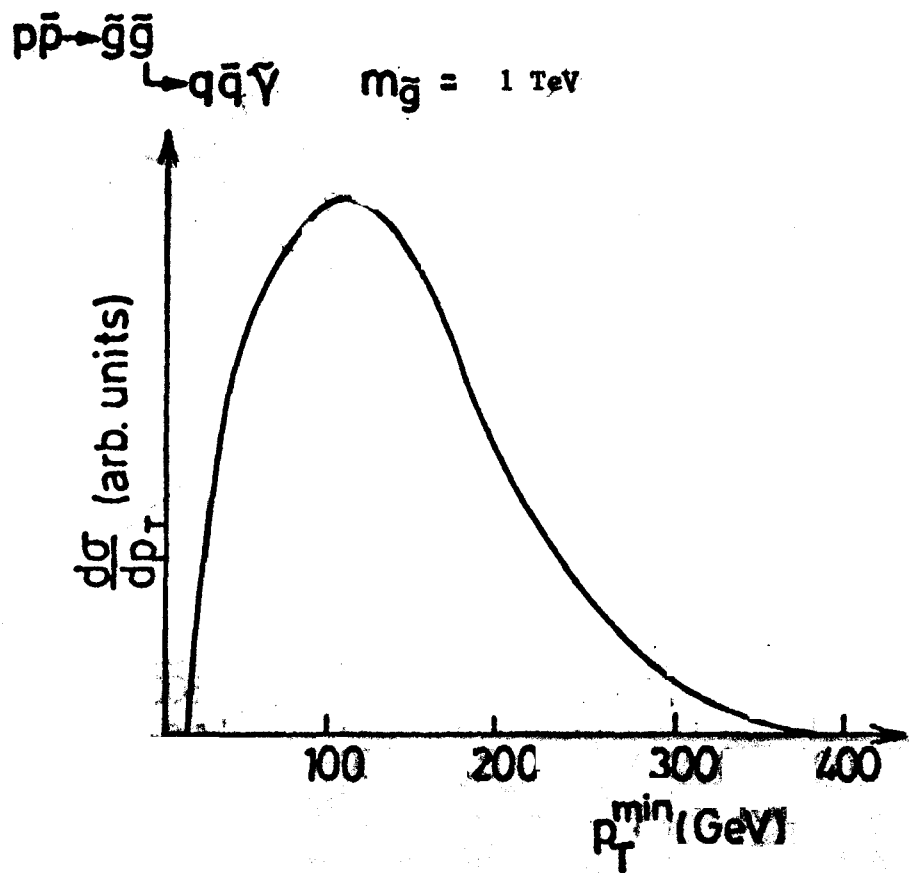


Fig. 16b

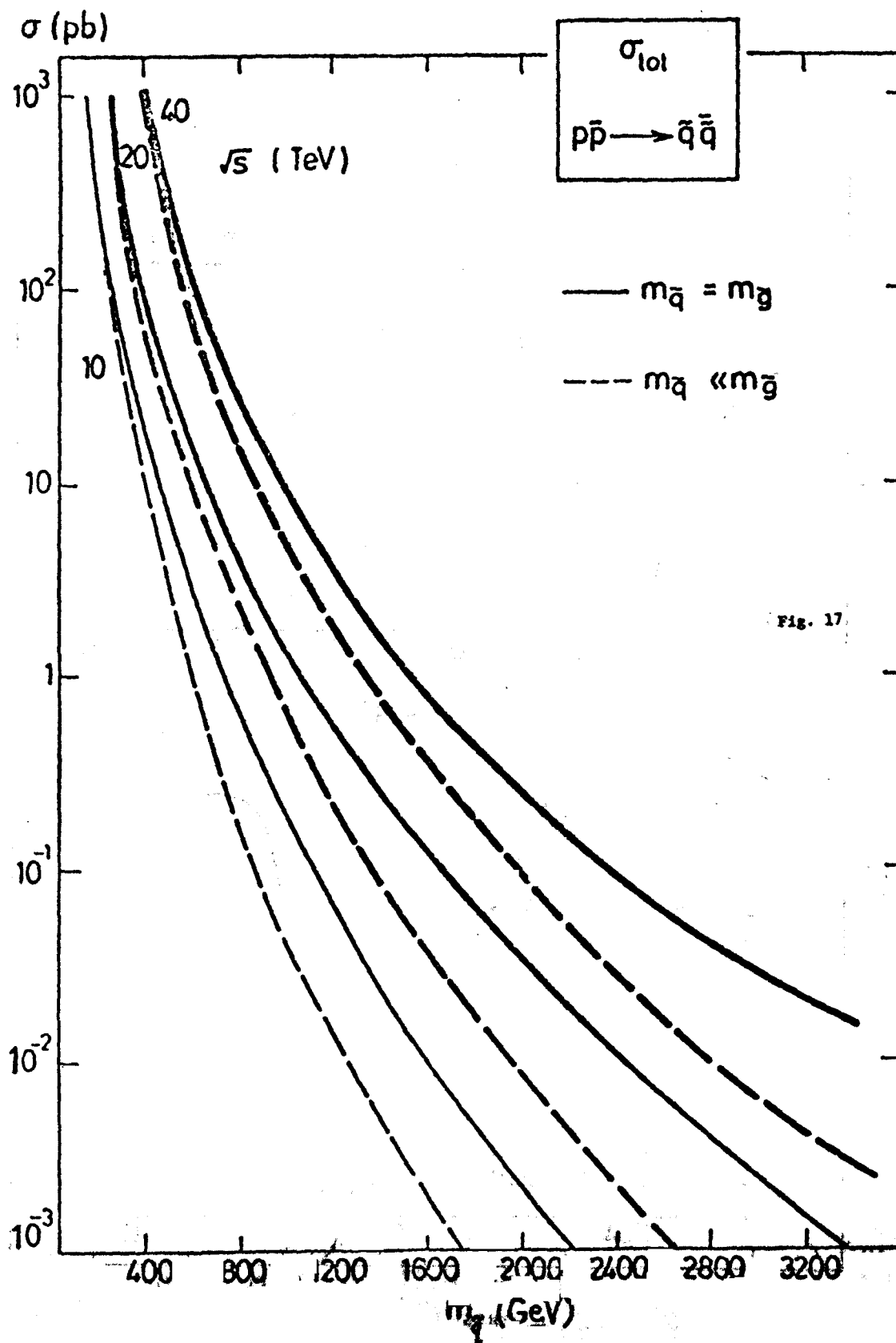


Fig. 17

Fig. 17

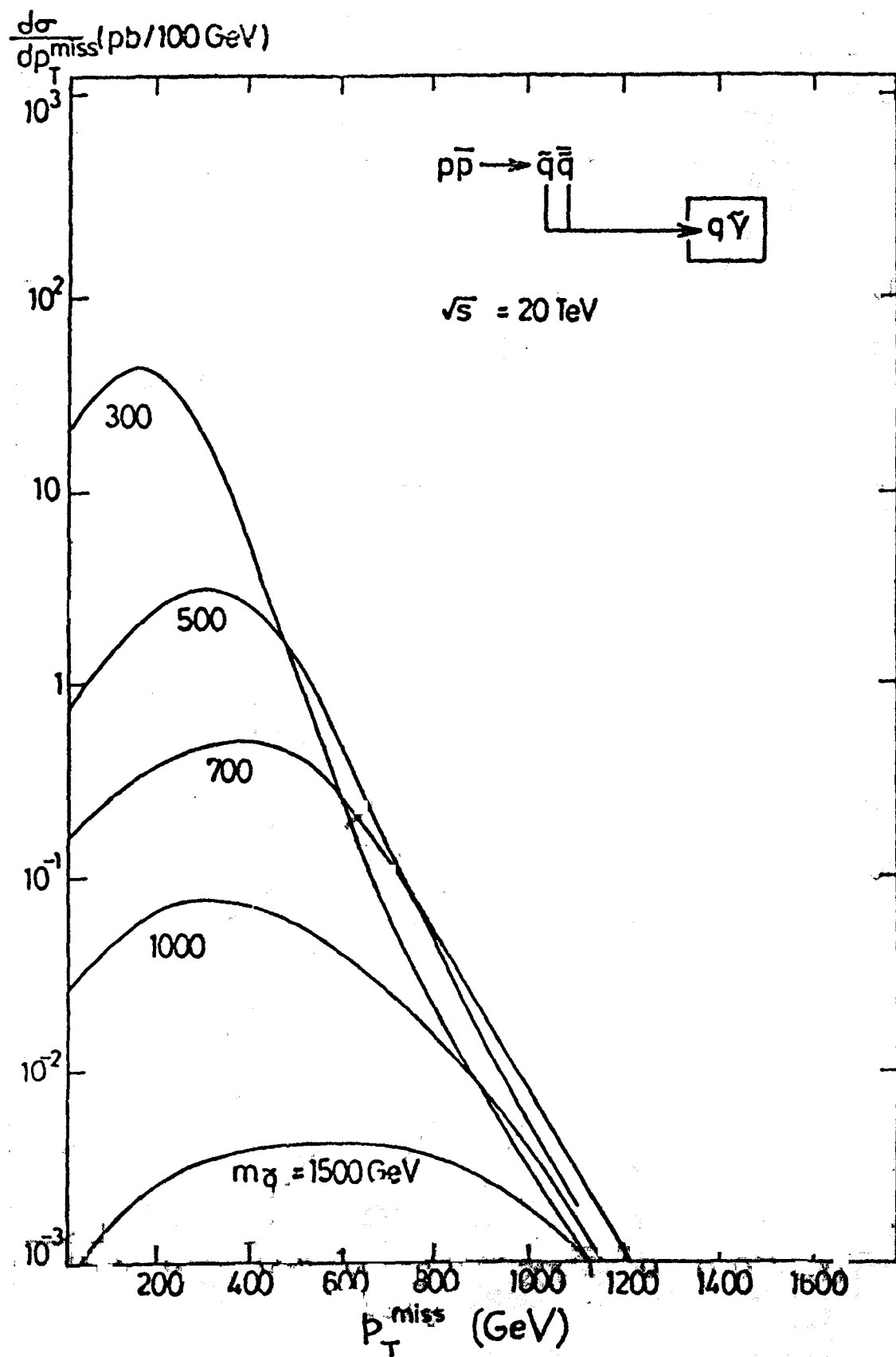
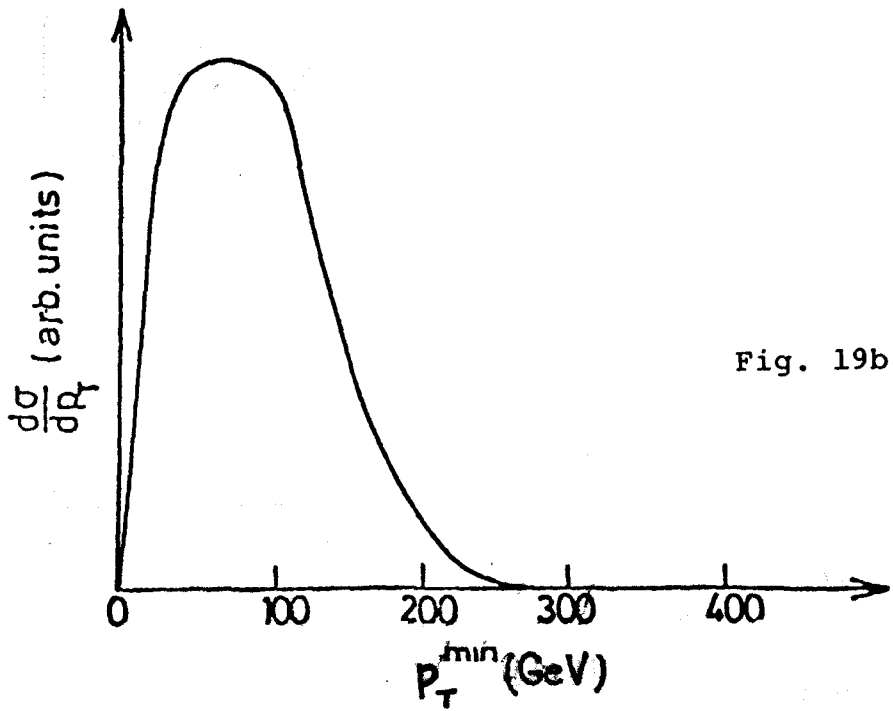
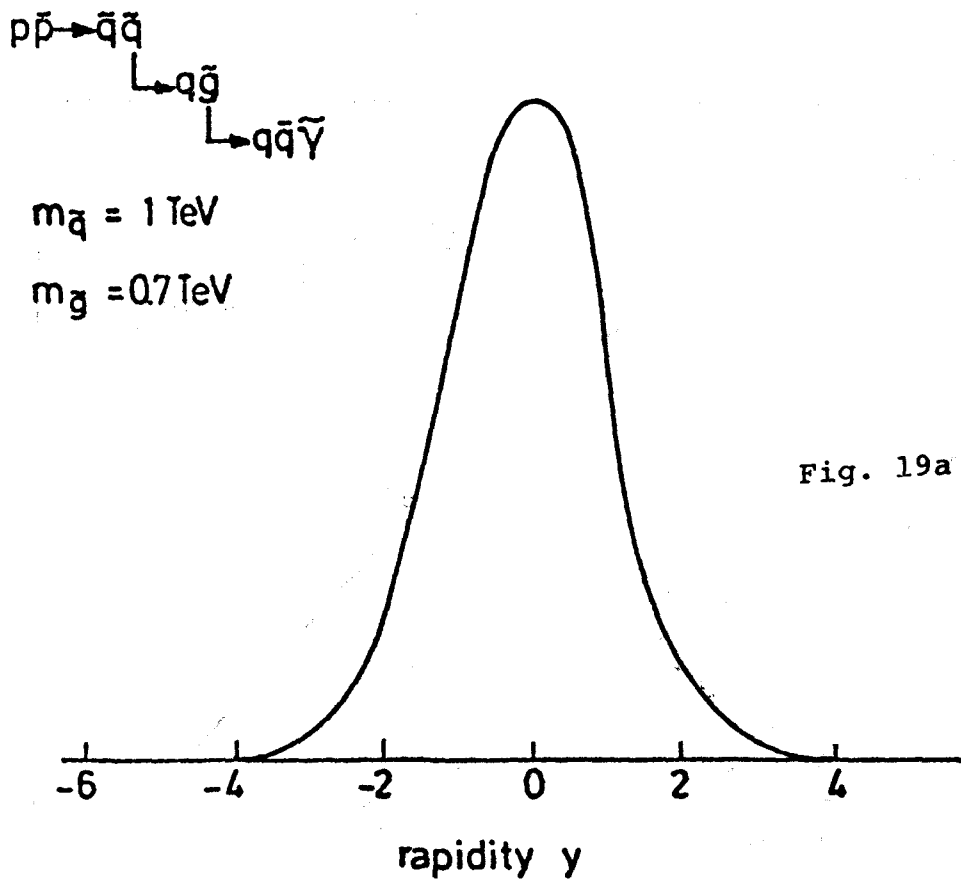


Fig. 18



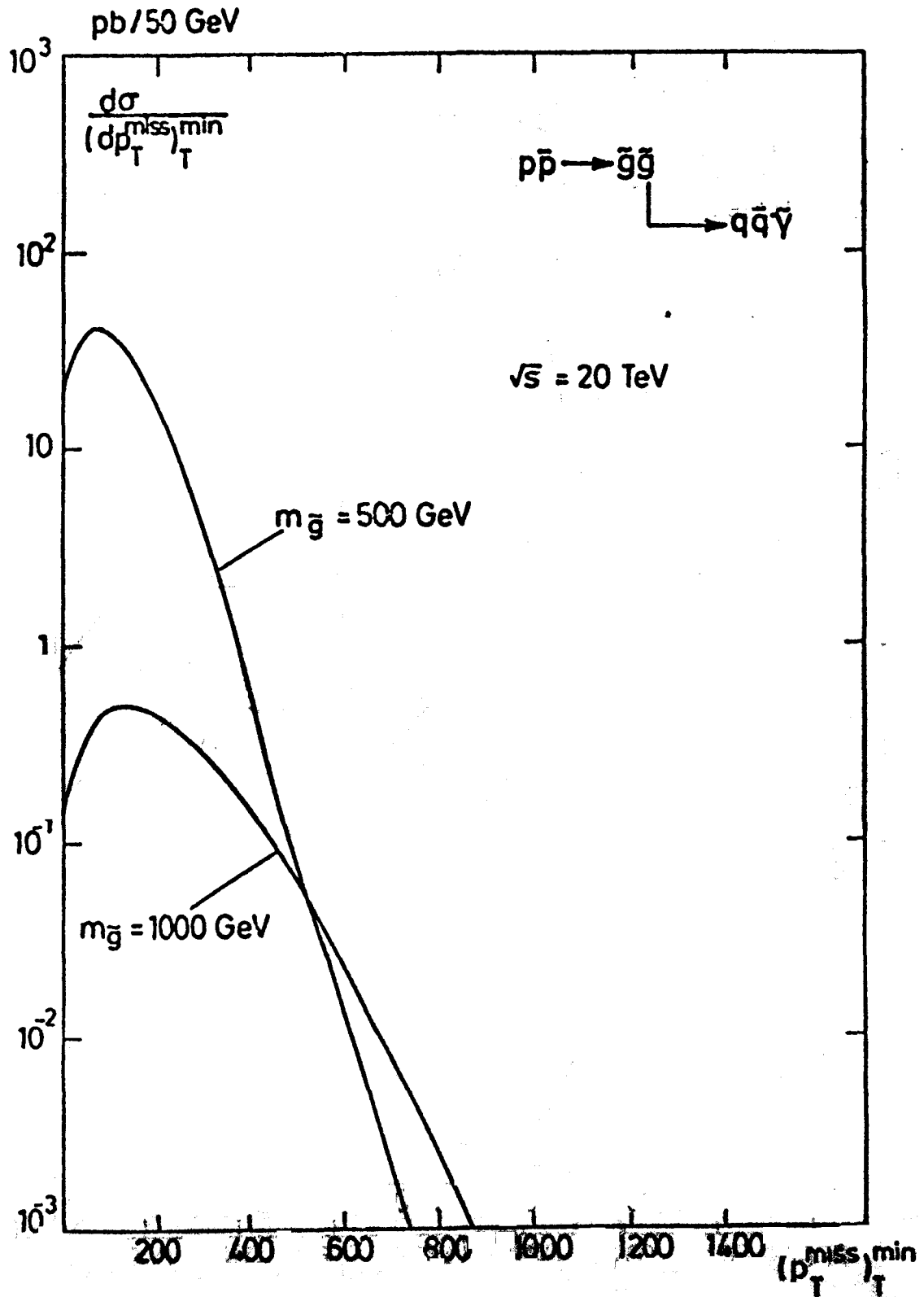


Fig. 20

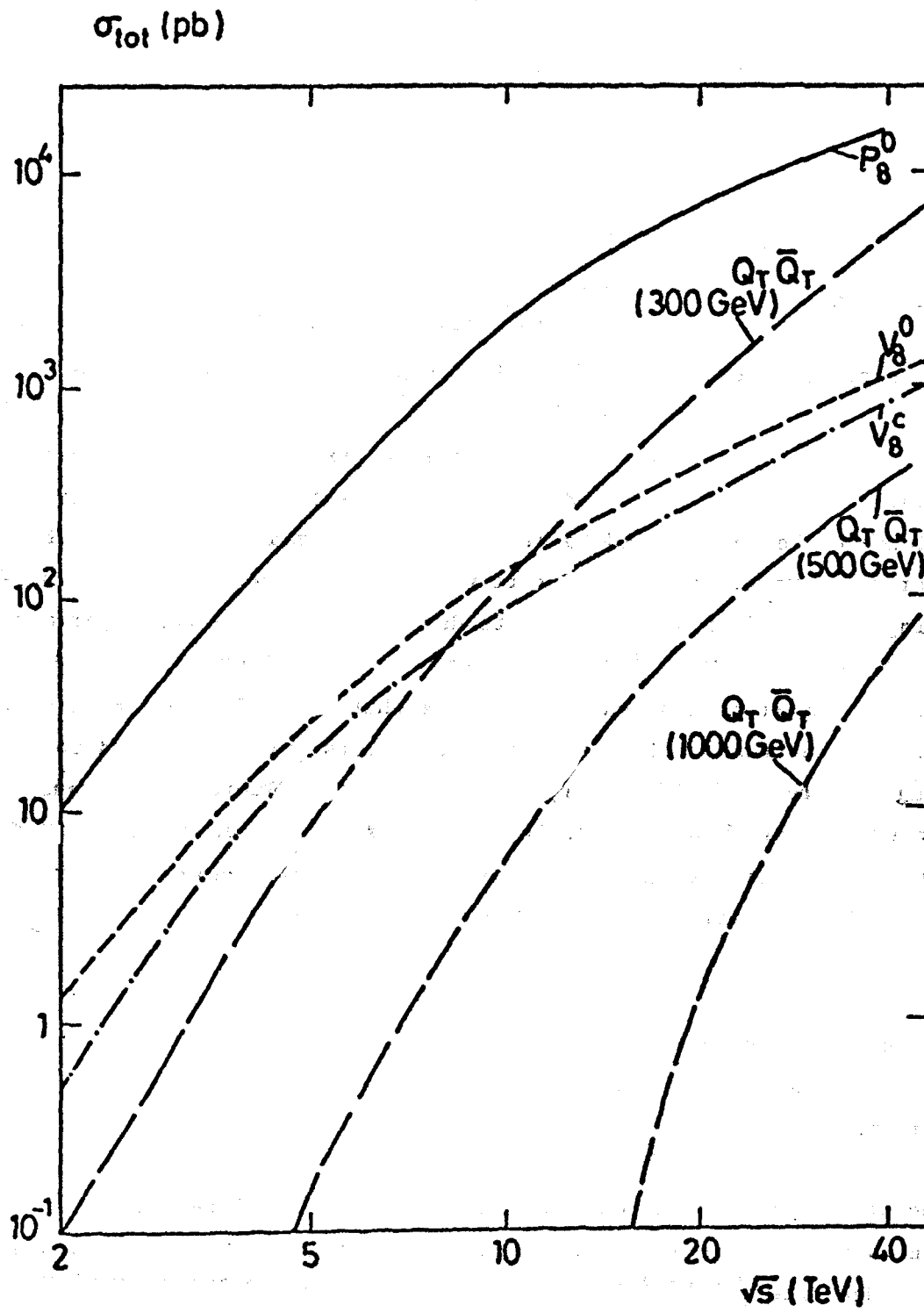


Fig. 21